PHYSICAL REVIEW B **107**, 075404 (2023)

Hartree method for molecular polaritons

Vladimir Al. Osipov [1,*] and Boris Fainberg [1,2,†]
[1] *H.I.T.-Holon Institute of Technology, 52 Golomb Street, POB 305, Holon 5810201, Israel*
[2] *School of Chemistry, Tel Aviv University, Tel Aviv 69978, Israel*

(Received 21 August 2022; revised 4 January 2023; accepted 17 January 2023; published 6 February 2023)

The formation of the composite photonic-excitonic particle, known as a polariton, is a phenomenon emerging in materials possessing strong coupling to light. The organic-based materials besides the strong light-matter coupling also demonstrate strong interaction of electronic and vibrational degrees of freedom. We study the vibration-assisted polariton wave-function evolution treating both types of interactions as equally strong. Using the multiconfiguration Hartree approach we derive the equations of motion for the polariton wave function, where the vibration degrees of freedom interact with the polariton quantum field through the mean-field Hartree term. For the conventional quadratic polariton Hamiltonian and the Holstein-type vibration Hamiltonian (Tavis-Cummings-Holstein model), the obtained equations are in one-to-one correspondence with the original Schrödinger equation. In the second part of the paper, we show that our theory reproduces the physical properties of the polariton light emission spectrum. In particular, the theory explains experimental observations of the molecular Stokes shift in the polariton fluorescence spectra in the systems with strong light-matter coupling. We also investigate the behavior of the polariton wave function in the vicinity of the anticrossing point and demonstrate that the Hartree term can produce an infinite potential barrier of a dynamical origin, which is responsible for the formation of the mixed upper-lower polariton states. The nonlinear nature of the polariton theory reflects their collective behavior. We expect that the multiconfiguration Hartree approach being applied to polaritons and similar systems will result in a manifestation of new physical phenomena.

DOI: 10.1103/PhysRevB.107.075404

I. INTRODUCTION

When dye molecules form a microstructure such as a nanofiber crystal [1], or a molecular solution placed into a microcavity, the strong light-matter interaction can lead to the formation of composite photon-exciton particles, known as exciton polaritons (see [2–5] and references therein). The systems with strong coupling to light draw a lot of attention due to their potential to cause changes in chemical reaction rates [6], to form high-temperature polariton Bose-Einstein condensate [3,7–9], and to show long-range particle propagation [1,10,11]. The concept, generally used to describe the polaritons in the organic-based devices, deals with the Frenkel excitons [12]. This type of excitons possesses the property to be localized on a few molecules (the typical size ∼10 Å), which, in particular, defines their stability (the binding energy ∼1 eV). A stronger coupling is achieved due to the large oscillator strength of the dye molecules. Entanglement of the excitonic states with certain light modes formed in the microcavity or with the free radiation modes splits the linearly growing with respect to the wave-vector-q light dispersion curve in the point of its crossing (the anticrossing point, AP) with almost constant exciton energy ω_{ex}. The gap width between the lower and the upper polariton dispersion branches (Rabi splitting) is governed by the strength of the light-matter interaction parameter g. In organic materials, g can reach significant values, up to 1 eV [1,4]. The above picture becomes more complex when one accounts for the interaction of the molecular electrons with the vibrational degrees of freedom, the inherent property of organic materials. The vibrations are known to assist the exciton-polariton stability and participate in such dynamic rearrangements of the polariton systems as Bose-type condensation [3], transport [1,11,13], and relaxation [14–18]. Therefore, when describing complex processes involving polaritons, both the interaction of light with molecules and the interaction of electron density with vibrations of the molecular cores must be treated on equal footing [19–24].

Vibrational degrees of freedom in crystals form the number of acoustic and optical phonon modes, which accounting is essential for describing semiconductor-based polaritonic devices. In the solutions of the organic dye molecules, the vibrations in the vicinity of each optically active center can be considered as if they were independent, and the other vibration degrees of freedom in the material or the solution effectively form a thermal bath. On the other hand, the large displacement of the equilibrium nuclear positions of the low-frequency optically active vibrations under the optical electronic transition leads to their excitation with large quantum numbers. In the monomolecular spectra, the low-frequency vibration modes reveal themselves in the Stokes shift between the emission and absorption peaks. The high-frequency optically active vibrations become visible in the form of the vibrational progression. Such strong effects must

---

[*] Vladimir.Al.Osipov@gmail.com

[†] Fainberg@hit.ac.il

also influence the polariton spectra. The influence of the high-frequency vibration modes on polaritons appeared to be more diverse. Its study led to some new interesting phenomena. The main peaks of the polariton fluorescent spectra are naturally associated with the energies of the upper and lower dispersions. The presence of the additional peaks and thermal broadening in the polariton spectra was studied in several works [16,25–27]. Recently, it was shown that the electron-vibrational interaction could result in the formation of the non-Markovian Fano resonances and the motional narrowing of the exciton-polariton luminescence spectrum [28]. In a number of papers, it was also shown that the molecular Stokes shift is one of the system parameters which can influence the polariton dynamics [17,29,30].

The approaches used to describe the polariton-vibration system were mainly based on phenomenological arguments. The aim of this research is in developing a rigorous, derived from first principles, approach for the description of the polariton-vibration system evolution. In particular, we study the vibration-assisted quantum evolution of the single-polariton wave function. It is worthy to note that for the solution of the transport problem, accounting of the polariton-polariton interaction [31], description of other dynamical processes [24], and also for developing of the multidimensional spectroscopy methods [18,32], the knowledge of the polariton wave-function evolution and its spatial propagation is of importance. A number of attempts to describe the polariton wave function have been done without accounting of vibrations [33,34]. In this paper, starting from the Tavis-Cummings-Holstein model Hamiltonian [35] we derive a set of equations for the polariton-vibration wave-function evolution in the Hartree approximation. Using these equations we consider several problems admitting approximate analytic solutions.

The vibronic coupling in a molecule interrelates the electronic and nuclear vibrational motion. In theoretical chemistry, the vibronic coupling is often neglected within the Born-Oppenheimer approximation. The couplings become crucial to the understanding of nonadiabatic processes, especially near AP, when the energy gap order of magnitude is comparable with the oscillation quantum energy. The large magnitude of the vibronic coupling near AP allows the wave function to propagate from one adiabatic potential energy surface to another, giving rise to a nonadiabatic phenomenon such as radiationless decay in molecular systems. The vibronic coupling can also form a singularity of the conical intersection type. This type of singularity is responsible for appearance of a nonzero geometric phase, which, in the context of molecular dynamics, was discovered by Longuet-Higgins [36]. In this case it becomes essential to account for the quantum interference of the system wave function with itself. In the context of the polariton-type systems, this effect was discussed in [37].

In our work, to describe the vibration degrees of freedom we use the language of coherent states. With a few relatively simple exceptions [38], the direct calculation of the quantum transitions assisted by vibrations within the coherent state framework [39] is not common due to the difficulties associated with their evaluation. To this end, several theoretical approaches have been developed, including the method of coupled coherent states [40]. The concept implies that the quantum trajectories are allowed to explore the phase space wider than the zero-vibration space. Having been equipped by a phase, the quantum trajectories start to interfere with each other. In this sense, the quantum effects can be thought of as arising from the interaction of the trajectories. This method belongs to a wider class of methods, which solve the Schrödinger equation in a time-dependent basis set and the time evolutions of both the basis vectors and that of the wave-function expansion coefficients are determined from the Dirac-Frenkel (sometimes Dirac-Frenkel and McLachlan) variational principle.

The coupled coherent states method is mainly used to describe the quantum evolution of a single molecule in an external field or without it. Contrary to the single-molecule models, the polariton quasiparticle is a composite particle and its quantum wave packet is spread over the whole microscopic sample (the polariton wavelength at AP is about 50 nm) and thus includes the quantum states of all molecules in the sample. The general nonlinear equations of polariton motion, obtained in the next section, include the forces acting from the side of each molecule on the polariton particle and also the backward action of the polariton on the molecular vibrations. Such a general model has to describe the whole variety of physical effects taking place in the system, including the effects of decoherence. The influence of different effects can be singled out by the special choice of the molecular Hamiltonian and, which is not less important, by an appropriate choice of the method for solving the nonlinear equation. In this paper, we use the multiconfiguration Hartree approach to formulate the equations of polariton motion in the mean-field approximation. In this approach the set of equations of motion split into two parts. The first part are the classical Newton equations, which describe the evolution of the vibration degrees of freedom. The presence of polaritons in this equation is taken into account by the Hartree term, which enters as a classical force resulting from the quantum averaging of the polariton field. The second part of the equations has the form of the Schrödinger equation written for the coefficients of the polariton wave-function expansion (they correspond to Hopfield coefficients in the standard polariton theory). These equations also contain a term proportional to the Hartree amplitude [41], which makes the equations essentially nonlinear. It turned out that the reformulation of the initial Schrödinger equation into the set of equations of the vibration-assisted polariton motion is exact in the case of the canonical quadratic polariton Hamiltonian and the Holstein-type vibration Hamiltonian [42]. The nonlinearity of the polariton equations reflects their collective behavior. We expect that the nonlinear effects can result in a manifestation of new physical phenomena in the polariton systems and also in similar multimolecular systems.

The paper is structured in the following way: In the next section (Sec. II), we derive equations of motion for the vibration-assisted polariton wave function. To do this, first (Sec. II A), we introduce the basis set of quantum polariton states for the quadratic polariton Hamiltonian without vibrations. To describe the vibrations in Sec. II B we introduce the basis of time-dependent coherent states. Varying the Schrödinger equation formulated for a model polariton-vibration Hamiltonian we derive the semiclassical equations of polariton evolution (Sec. II C). In Sec. III A we solve the system of polariton equations of motion in the quasidiagonal approximation to calculate the polariton fluorescent spectrum, some details of calculation are given in Appendices A and C. The equations of motion in the vicinity of AP and also dynamical formation of a potential barrier separating the mixed states from the pure polariton states are discussed in Sec. III B. The results of our research are discussed in Sec. IV.

II. EQUATIONS OF MOTION FOR THE VIBRATION-ASSISTED POLARITON WAVE FUNCTION

A. Basis set of the polariton Hamiltonian

In this work, we focus on the type of systems in which in the first approximation the dipole-dipole interactions between molecules can be neglected. An example of such a system is the solution of enhanced green fluorescent protein (eGFP). The actual fluorophore of FPs is enclosed by a nanocylinder that consists of 11 β sheets [43,44]. This protective shell acts as a natural "bumper" and prevents close contact between fluorophores of neighboring FPs, limiting the intermolecular energy migration even at the highest possible concentration. The intermolecular interactions impart [45] the momentum q dependence to the exciton dispersion $\omega_{\rm ex}$. In the case of weakly coupled molecules the short-range Frenkel exciton effective mass is large and we can neglect the q dependence in $\omega_{\rm ex}$. Note that there are examples of systems, where the dipole-dipole interaction (excitonic coupling) is suppressed even in the crystal phase [44,46,47]. To this end, we also add that below we consider the polariton operators as those that satisfy the Bose statistics, which is an assumption taking place at a low density of excitations. Discussion regarding the admissibility of such approximation one can find in Refs. [48,49]. It was shown there that the composite nature of the Frenkel excitons is responsible for the excitation transfer. In what follows, we consider a single-polariton wave function when the nonbosonic corrections nullify.

In this section, we introduce the polariton basis vector set for the basic model of the polariton Hamiltonian $\hat{H}_{\rm pol}$. For systems without any distinguished spatial directions when the light scattering from the inhomogeneities of the medium can be neglected, one can work with the basic model polariton Hamiltonian $\hat{H}_{\rm pol}$, which diagonalized form is quadratic in the upper, Q_q, and the lower, P_q, polariton operators [50]:

$$\hat{H}_{\rm pol} = \hbar \sum_q \Lambda_{+q} Q_q^\dagger Q_q + \Lambda_{-q} P_q^\dagger P_q. \tag{1}$$

The polariton operators and the polariton energies, $\Lambda_{\pm q}$, depend on the wave vector q. The polariton dispersion relations are known to be the solution of a quadratic equation and expressed in terms of the exciton energy $\omega_{\rm ex}$ and the photon energy ω_q:

$$\Lambda_{\pm q} = \tfrac{1}{2}\left(\omega_q + \omega_{\rm ex} \pm \sqrt{(\omega_q - \omega_{\rm ex})^2 + 4g^2}\right). \tag{2}$$

The Rabi splitting, i.e., the width of the gap between the upper and the lower polariton branches, is governed by the light-matter interaction strength constant g. The polariton operators Q_q and P_q are expressed in terms of the material operators by means of the unitary transformation parametrized by the "Hopfield angle" ϕ_q [see Fig. 1(b)],

$$Q_q = \cos\phi_q A_q - i\,\sin\phi_q \frac{1}{\sqrt{N}} \sum_m e^{-iqm} b_m, \tag{3}$$

$$P_q = \sin\phi_q A_q + i\,\cos\phi_q \frac{1}{\sqrt{N}} \sum_m e^{-iqm} b_m, \tag{4}$$

where N is the total number of molecules and qm denotes the scalar product of the wave vector q and the radius-vector pointing at the optical transition center of the mth molecule. The operators A_q in Eqs. (3) and (4) are the boson annihilation operators of a photon in the mode q. The operators b_m are the annihilation operators of the excited state at the mth molecule. The exciton annihilation and creation operators are

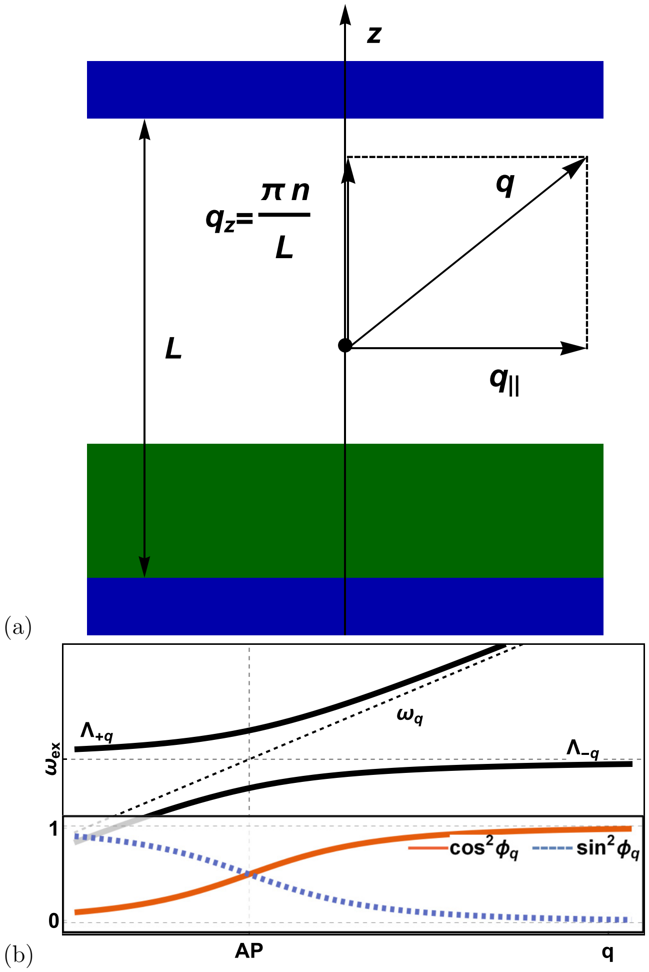

FIG. 1. (a) The molecular substance (green area) containing a thin layer of the molecular solution is placed between two cavity mirrors (blue rectangles) with the distance L between them. The light modes formed in the microcavity have the wave vector q with the in-plane $q_\parallel$ and transverse q_z components $q = (q_\parallel, q_z)$. The transverse component q_z can have only discrete values marked by $n = 1, 2, \ldots$. (b) The polariton dispersion curves $\Lambda_{\pm q}$ and the Hopfield coefficients $\cos^2\phi_q$, $\sin^2\phi_q$ (in the insert) plotted vs the wave vector q. AP denotes the anticrossing point $\omega_{\rm ex} = \omega_q$.

known to be Paulions (or composite bosons, according to the terminology used in Refs. [48,49]): they possess the fermion properties $[b_m, b_m^\dagger]_+ = 1$ at one and the same site, and commute for different sites $[b_m, b_{m'}^\dagger] = 0$ when $m \neq m'$. Under the assumption of a small density of the excitations, the operators b_m approximately (up to the order 1/N) satisfy the bosonic commutation relations $[b_m, b_{m'}^\dagger] = \delta_{m,m'}$, and so do the polariton operators $[Q_q, Q_{q'}^\dagger] = [P_q, P_{q'}^\dagger] = \delta_{q,q'}$. The substitution of Paulions by bosons for small excitation densities historically can be traced back to the method of approximate second quantization developed in the theory of magnetism [51]. The Paulion state can be either occupied or unoccupied, whereas the occupation numbers for bosons can be any positive integer number. Therefore, the replacement of Paulions by bosons fails when the number of bosons is larger than 1. In the case of nonlinear optical effects this is avoided by adding into the quadratic "boson" Hamiltonian [Eq. (1)] the operator of kinematic interaction, which includes the terms of the fourth and higher orders [12,52,53]. The operator of kinematic interaction results in a nonlinear interaction between the bosons. In this relation, a useful and straightforward method for accounting of the multi-Frenkel exciton states can be found in Refs. [48,49]. In our theory, where the interaction between polaritons is caused by vibrations, the nonlinear equations appear even for the single-polariton state describing the single-exciton processes. The solution of nonlinear equations is a nontrivial problem by itself, so to focus on a new physics related to our nonlinear theory, we exclude the additional nonlinearities generated by the multiexciton states in the nonlinear optical processes. Thus, we restrict the application of our theory to the linear optical processes for which it is sufficient to take into account the single-exciton states.

A few remarks have to be made at this point:

(1) The Hopfield angle ϕ_q in Eqs. (3) and (4) is defined through the relation $\cos 2\phi_q = \frac{\omega_q - \omega_{\rm ex}}{\Lambda_{+q} - \Lambda_{-q}}$. Its value ranges from 0 at large q, $q \to \infty$, to some value close but smaller than $\pi/2$ at $q = 0$. The wave vector satisfying the AP position $\omega_q = \omega_{\rm ex}$ corresponds to $\phi_q = \pi/4$.

(2) The problem implies the symmetry with respect to the generic change of the momentum sign, so that all the equations have to be invariant under the transformation $q \to -q$, and, in particular, $\omega_q = \omega_{-q}$ and $\phi_q = \phi_{-q}$.

(3) In our formulation we use the rescaling, where m is an integer-valued vector and the dimension units are absorbed by the wave vector q and also by the energy units. In the free space the photons dispersion ω_q is linear in the wave-vector absolute value. In our notations the free-space photon energy has the form $\omega_q = c|q|/n_0\langle\ell\rangle$, where c/n_0 is the speed of light in the medium and $\langle\ell\rangle$ is the mean distance between the molecules. Below, for convenience, we omit $\langle\ell\rangle$, bearing in mind that $\langle\ell\rangle$ is canceled in the final formulas, and q is measured in conventional units. In the case when the active media are placed into a microcavity the wave-vector values are bounded from below by the wave vector q_z of the eigenmode excited in the resonator and $\omega_q = \frac{c}{n_0}\sqrt{q_z^2 + q_\parallel^2}$ (see Fig. 1).

(4) The single-polariton states of the polariton Hamiltonian $\hat{H}_{\rm pol}$ [Eq. (1)] are composed of the vectors which we denote by $|q, u\rangle$. They are distinguished by the parameters q, u. Each of $|q, u\rangle$ describes an upper ($u = 1$) or lower ($u = 0$) polariton excited with the momentum q,

$$|q, 0\rangle = P_q^\dagger\,|0\rangle\,, \quad |q, 1\rangle = Q_q^\dagger\,|0\rangle\,. \tag{5}$$

The vector $|0\rangle$ denotes the ground state of the system with zero polaritons. The nonzero matrix elements of the polariton Hamiltonian are

$$\langle q, u|\,\hat{H}_{\rm pol}\,|q, u\rangle = (1-u)\Lambda_{-q} + u\Lambda_{+q}. \tag{6}$$

(5) Accounting of the vibrations shifts the energy of the molecular optical transition by half of the Stokes shift $\omega_{\rm St}/2$. In the next section (Sec. II B) it is implied that $\omega_{\rm ex} \to \omega_{\rm ex} + \omega_{\rm St}/2$ in Eq. (2) and in the related equations.

B. Vibration Hamiltonian and the extended basis set of the polariton wave functions

The total Hamiltonian of the molecular system with polaritons $\hat{\mathcal{H}}$ contains two contributions: the polariton part $\hat{H}_{\rm pol}$, which was discussed in the previous section [Eq. (1)], and the vibrational part $\hat{H}_{\rm vib}$, which describes interaction of electrons with vibrations:

$$\hat{\mathcal{H}} = \hat{H}_{\rm pol} + \hat{H}_{\rm vib}. \tag{7}$$

The vibrational part of the Hamiltonian is modeled by the standard electron-vibration Holstein-type [42] Hamiltonian

$$\begin{aligned}\hat{H}_{\rm vib} = \sum_{m,\mu}[&\hat{H}_{\rm bath}(c_{m,\mu}^\dagger, c_{m,\mu}) + \hbar\Omega_\mu c_{m,\mu}^\dagger c_{m,\mu}\\ &- \hbar\Omega_\mu X_\mu(c_{m,\mu}^\dagger + c_{m,\mu})b_m^\dagger b_m].\end{aligned} \tag{8}$$

It is assumed that the electron transition in the mth molecule is coupled to a number of quantum harmonic oscillations of the molecular backbone with various energy quanta $\hbar\Omega_\mu$ indexed by $\mu = 0, 1, \ldots$. The frequencies Ω_μ and the oscillator equilibrium coordinate shifts X_μ in the excited electronic state are equal for all molecules. The optically active vibration modes (boson operators $c_{m,\mu}$ and $c_{m,\mu}^\dagger$, $[c_{m,\mu}, c_{m',\mu'}^\dagger] = \delta_{m,m'}\delta_{\mu,\mu'}$) interact with the dark modes via the thermal bath Hamiltonian $\hat{H}_{\rm bath}$. We assume that this term also includes, if necessary, the interactions of vibrations localized at different molecules. Remind here that the excitation energy has to be shifted by the half of the Stokes shift $\omega_{\rm St} \equiv 2\sum_\mu \Omega_\mu X_\mu^2$, i.e., we imply that $\omega_{\rm ex} \to \omega_{\rm ex} + \omega_{\rm St}/2$ in Eq. (2) and in the related equations.

The basis of coherent states provides a convenient description for vibration degrees of freedom [39]. Each coherent state $|\sigma\rangle$ is parametrized by multidimensional complex-valued vector σ. It encodes the coherent state center, i.e., the classical coordinate x and the classical momentum p, namely, $\sigma = x + ip$. The vibration operators act on the basis vectors as follows: $c\,|\sigma\rangle = \sigma\,|\sigma\rangle$, $\langle\sigma|\,c^\dagger = \langle\sigma|\,\sigma^*$ and the normalized coherent state have the representation

$$|\sigma\rangle = e^{-\frac{1}{2}|\sigma|^2} e^{\sigma c^\dagger}\,|0\rangle\,, \tag{9}$$

where $|0\rangle$ is the ground state of the corresponding oscillator.

As we mentioned in the previous section, we consider only the single-polariton state, which is described by two types of vectors: $|q, 0\rangle$, and $|q, 1\rangle$. Thus, our working basis consists of the direct products of the polariton and vibrational states

$(u = 0, 1)$

$$|\boldsymbol{\sigma}, q, u\rangle = |\boldsymbol{\sigma}\rangle\, |q, u\rangle\,, \qquad |\boldsymbol{\sigma}\rangle = \bigotimes_{m,\mu} |\sigma_{m,\mu}\rangle\,. \tag{10}$$

The scalar product of the vectors defined above is

$$\begin{aligned} \langle \boldsymbol{\sigma}', q', u' | \boldsymbol{\sigma}, q, u\rangle &= \langle \boldsymbol{\sigma}' | \boldsymbol{\sigma}\rangle\, \langle q', u' | q, u\rangle \\ &= \exp\left(-\frac{1}{2} \sum_{m,\mu} |\sigma'_{m,\mu} - \sigma_{m,\mu}|^2 \right) \delta_{q',q}\delta_{u',u}. \end{aligned} \tag{11}$$

The completeness and orthogonality relation for the extended basis [Eq. (10)] takes the form

$$\mathbb{1} = \sum_{\boldsymbol{\sigma}} \sum_{q} \sum_{u=0,1} |\boldsymbol{\sigma}, q, u\rangle\, \langle \boldsymbol{\sigma}, q, u|\,. \tag{12}$$

Here and below the sum $\sum_{\boldsymbol{\sigma}}$ denotes the integration $\int d^2\sigma_{m,\mu}/\pi$ over each component of the vector $\boldsymbol{\sigma}$.

C. Polariton wave-function evolution in the time-dependent basis and equations of motion

The basis of vectors [Eq. (10)] defined in the previous section does not diagonalize the total Hamiltonian $\hat{\mathcal{H}}$. To describe the evolution of the wave function we make use an anzatz, which states that the basis of the coherent states is time dependent, i.e., in addition to the time dependence of the expansion coefficients $\mathcal{C}(\boldsymbol{\sigma}, q, u|t)$, we assume that the basis vectors also depend on time, $|\boldsymbol{\sigma}(t), q, u\rangle$. The wave function of the system can be standardly expanded in this basis

$$|\Psi(t)\rangle = \sum_{\boldsymbol{\sigma},q,u} \mathcal{C}(\boldsymbol{\sigma}, q, u|t)\, |\boldsymbol{\sigma}(t), q, u\rangle\,. \tag{13}$$

To work with such wave functions we use the approach which is based on the Dirac-Frenkel variation principle. This approach is known to be useful for the description of quantum dynamics in systems with a large number of vibration degrees of freedom [40,54–56]. In our case it allows us to separate the time evolution of the vibration subsystem and the quantum evolution of the polariton wave function. The wave-function (13) variation is

$$\begin{aligned} \langle \delta\Psi(t)| = \sum_{\sigma,q,u} \langle \boldsymbol{\sigma}, q, u| \Bigg\{ &\delta\mathcal{C}^*(\boldsymbol{\sigma}, q, u|t) + \mathcal{C}^*(\boldsymbol{\sigma}, q, u|t) \\ &\times \sum_{m,\mu} \left(\delta\sigma^*_{m,\mu} c_{m,\mu} - \frac{1}{2}[\sigma_{m,\mu}\delta\sigma^*_{m,\mu} + \sigma^*_{m,\mu}\delta\sigma_{m,\mu}] \right) \Bigg\}. \end{aligned} \tag{14}$$

The second term in Eq. (14) results from the variation of the coherent state written in the form (9). Variation of the Schrödinger equation $\langle \Psi|\, i\hbar\frac{d}{dt} - \hat{\mathcal{H}}\, |\Psi\rangle = 0$ with respect to the bra-vector and equating to zero each term proportional to the independent variations $\delta\mathcal{C}(\boldsymbol{\sigma}', q', u'|t)$, and $\delta\sigma_{m,\mu}$ yields the system of coupled equations,

$$\langle \boldsymbol{\sigma}', q', u'|\, i\hbar\frac{d}{dt} - \hat{\mathcal{H}}\, |\Psi\rangle = 0, \tag{15}$$

$$\mathcal{C}^*(\boldsymbol{\sigma}', q', u'|t)\, \langle \boldsymbol{\sigma}', q', u'|\, c_{m,\mu} \left(i\hbar\frac{d}{dt} - \hat{\mathcal{H}} \right) |\Psi\rangle = 0. \tag{16}$$

From Eq. (14) we also derive the expression for the time derivative of the wave function,

$$\begin{aligned} \frac{d}{dt}\, |\Psi(t)\rangle = \sum_{\sigma,q,u} \Bigg\{ &\dot{\mathcal{C}}(\boldsymbol{\sigma}, q, u|t) + \mathcal{C}(\boldsymbol{\sigma}, q, u|t) \sum_{m,\mu} \Bigg(\dot{\sigma}_{m,\mu} c^\dagger_{m,\mu} \\ &- \frac{1}{2}[\sigma_{m,\mu}\dot{\sigma}^*_{m,\mu} + \sigma^*_{m,\mu}\dot{\sigma}_{m,\mu}] \Bigg) \Bigg\}\, |\boldsymbol{\sigma}, q, u\rangle\,. \end{aligned} \tag{17}$$

The overdot symbol, as usual, denotes the time derivative. Substitution of the above expression [Eq. (17)] into Eqs. (15) and (16) leads to two equations which extended forms are

$$\begin{aligned} \sum_{\boldsymbol{\sigma}} \langle \boldsymbol{\sigma}' | \boldsymbol{\sigma}\rangle\, \dot{\mathcal{C}}(\boldsymbol{\sigma}, q', u'|t) = &-\frac{i}{\hbar} \sum_{\boldsymbol{\sigma},q,u} \langle \boldsymbol{\sigma}', q', u'|\, \hat{\mathcal{H}}\, |\boldsymbol{\sigma}, q, u\rangle\, \mathcal{C}(\boldsymbol{\sigma}, q, u|t) + \frac{1}{2} \sum_{\boldsymbol{\sigma}} \langle \boldsymbol{\sigma}' | \boldsymbol{\sigma}\rangle\, \mathcal{C}(\boldsymbol{\sigma}, q', u'|t) \sum_{m,\mu} [\sigma_{m,\mu}\dot{\sigma}^*_{m,\mu} - \sigma^*_{m,\mu}\dot{\sigma}_{m,\mu}] \\ &- \sum_{\boldsymbol{\sigma}} \langle \boldsymbol{\sigma}' | \boldsymbol{\sigma}\rangle\, \mathcal{C}(\boldsymbol{\sigma}, q', u'|t) \sum_{m,\mu} (\sigma'^*_{m,\mu} - \sigma^*_{m,\mu})\dot{\sigma}_{m,\mu}, \end{aligned} \tag{18}$$

$$\begin{aligned} &\mathcal{C}^*(\boldsymbol{\sigma}', q', u'|t) \sum_{\sigma} \langle \boldsymbol{\sigma}' | \boldsymbol{\sigma}\rangle\, [\sigma_{m,\mu}\dot{\mathcal{C}}(\boldsymbol{\sigma}, q', u'|t) + \dot{\sigma}_{m,\mu}\mathcal{C}(\boldsymbol{\sigma}, q', u'|t)] \\ &\quad = -\frac{i}{\hbar}\mathcal{C}^*(\boldsymbol{\sigma}', q', u'|t) \sum_{\boldsymbol{\sigma},q,u} \langle \boldsymbol{\sigma}', q', u'|\, c_{m,\mu}\hat{\mathcal{H}}\, |\boldsymbol{\sigma}, q, u\rangle\, \mathcal{C}(\boldsymbol{\sigma}, q, u|t) + \frac{1}{2}\mathcal{C}^*(\boldsymbol{\sigma}', q', u'|t) \sum_{\boldsymbol{\sigma}} \langle \boldsymbol{\sigma}' | \boldsymbol{\sigma}\rangle\, \sigma_{m,\mu}\mathcal{C}(\boldsymbol{\sigma}, q', u'|t) \\ &\quad\quad \times \sum_{n,\nu} ([\sigma_{n,\nu}\dot{\sigma}^*_{n,\nu} - \sigma^*_{n,\nu}\dot{\sigma}_{n,\nu}] - 2(\sigma'^*_{n,\nu} - \sigma^*_{n,\nu})\dot{\sigma}_{n,\nu}). \end{aligned} \tag{19}$$

Now we have to specify the terms including the Hamiltonian $\hat{\mathcal{H}}$. The system Hamiltonian $\hat{\mathcal{H}}$ consists of two parts $\hat{H}_{\text{pol}}$ and $\hat{H}_{\text{vib}}$. The polariton Hamiltonian (1) is diagonalized in the basis (10), its nonzero entries are

$$\begin{aligned} \langle \boldsymbol{\sigma}', q', u'|\, \hat{H}_{\text{pol}}\, |\boldsymbol{\sigma}, q, u\rangle = \hbar\, &\langle \boldsymbol{\sigma}' | \boldsymbol{\sigma}\rangle\, \delta_{q',q}\delta_{u',u} \\ &\times [(1-u)\Lambda_{-q} + u\Lambda_{+q}], \end{aligned} \tag{20}$$

$$\begin{aligned} \langle \boldsymbol{\sigma}', q', u'|\, c_{m,\mu}\hat{H}_{\text{pol}}\, |\boldsymbol{\sigma}, q, u\rangle = \sigma_{m,\mu}\hbar\, &\langle \boldsymbol{\sigma}' | \boldsymbol{\sigma}\rangle\, \delta_{q',q}\delta_{u',u} \\ &\times [(1-u)\Lambda_{-q} + u\Lambda_{+q}]. \end{aligned} \tag{21}$$

To continue our calculations we make use the general observation that the matrix elements $\langle \boldsymbol{\sigma}', q', u'|\, \hat{\mathcal{H}}\, |\boldsymbol{\sigma}, q, u\rangle$ of a generic normally ordered in $c^\dagger_{m,\mu}$ and $c_{m,\mu}$ Hamiltonian $\hat{\mathcal{H}}$ can be obtained by replacing of $c^\dagger_{m,\mu}$ and $c_{m,\mu}$ by ${\sigma'_{m,\mu}}^*$ and $\sigma_{m,\mu}$, respectively, i.e.,

$$\langle \boldsymbol{\sigma}', q', u'|\, \hat{\mathcal{H}}\, |\boldsymbol{\sigma}, q, u\rangle = \langle \boldsymbol{\sigma}'|\boldsymbol{\sigma}\rangle\, \langle q', u'|\, \hat{\mathcal{H}}(\boldsymbol{\sigma}'^{*}, \boldsymbol{\sigma})\, |q, u\rangle \tag{22}$$

and correspondingly

$$\begin{aligned}\langle \boldsymbol{\sigma}', q', u'|\, c_{m,\mu}\hat{\mathcal{H}}\, |\boldsymbol{\sigma}, q, u\rangle - \sigma_{m,\mu}\, \langle \boldsymbol{\sigma}', q', u'|\, \hat{\mathcal{H}}\, |\boldsymbol{\sigma}, q, u\rangle \\ = \langle \boldsymbol{\sigma}'|\boldsymbol{\sigma}\rangle\, \frac{\partial}{\partial {\sigma'_{m,\mu}}^{*}}\, \langle q', u'|\, \hat{\mathcal{H}}(\boldsymbol{\sigma}'^{*}, \boldsymbol{\sigma})\, |q, u\rangle\, .\end{aligned} \tag{23}$$

The matrix elements of the vibration Hamiltonian can be calculated with the help of Eqs. (3) and (4). The electron operators expressed in terms of the polariton operators yield

$$\begin{aligned} b^\dagger_m b_m = \frac{1}{N}\sum_{q',q} e^{-i(q'-q)m}(\sin\phi_{q'} Q^\dagger_{q'} - \cos\phi_{q'} P^\dagger_{q'}) \\ \times (\sin\phi_q Q_q - \cos\phi_q P_q).\end{aligned} \tag{24}$$

The matrix elements of the polariton operator products are calculated from Eq. (5), namely,

$$\langle q', u'|\, Q^\dagger_{s'} Q_s\, |q, u\rangle = u\, \delta_{u',u}\delta_{s',q'}\delta_{s,q}, \tag{25}$$

$$\langle q', u'|\, P^\dagger_{s'} P_s\, |q, u\rangle = (1-u)\, \delta_{u',u}\delta_{s',q'}\delta_{s,q}, \tag{26}$$

$$\langle q', u'|\, P^\dagger_{s'} Q_s\, |q, u\rangle = u(1-u')\, \delta_{s',q'}\delta_{s,q}, \tag{27}$$

$$\langle q', u'|\, Q^\dagger_{s'} P_s\, |q, u\rangle = u'(1-u)\, \delta_{s',q'}\delta_{s,q}. \tag{28}$$

Note that the indices s and s' are not necessarily equal so that each of the above operator products is responsible for the polariton annihilation in some mode q and its creation in some other mode q' or in the same mode q when $s' = s$.

Combining all results we derive the matrix elements of the vibration Hamiltonian

$$\begin{aligned}\langle \boldsymbol{\sigma}', q', u'|\, \hat{H}_{\text{vib}}\, |\boldsymbol{\sigma}, q, u\rangle = -\, \langle \boldsymbol{\sigma}'\boldsymbol{\sigma}\rangle \sum_{m,\mu} \frac{\hbar\Omega_\mu X_\mu}{N}({\sigma'_{m,\mu}}^{*} + \sigma_{m,\mu})e^{-i(q'-q)m}[\boldsymbol{v}_{q',q}]_{u',u} + \langle \boldsymbol{\sigma}'|\boldsymbol{\sigma}\rangle\, \delta_{q',q}\delta_{u',u}\hbar \sum_{m,\mu}\Omega_\mu {\sigma'_{m,\mu}}^{*}\sigma_{m,\mu} \\ + \langle \boldsymbol{\sigma}'|\boldsymbol{\sigma}\rangle\, \delta_{q',q}\delta_{u',u} H_{\text{bath}}(\boldsymbol{\sigma}'^{*}, \boldsymbol{\sigma}),\end{aligned} \tag{29}$$

where $[\boldsymbol{v}_{q',q}]_{u',u}$ denotes the (u', u) component of the matrix of the Hopfield coefficients $\boldsymbol{v}_{q',q}$,

$$\boldsymbol{v}_{q',q} = \begin{pmatrix} [\boldsymbol{v}_{q',q}]_{1,1} & [\boldsymbol{v}_{q',q}]_{1,0} \\ [\boldsymbol{v}_{q',q}]_{0,1} & [\boldsymbol{v}_{q',q}]_{0,0}\end{pmatrix} \equiv \begin{pmatrix} \sin\phi_{q'}\sin\phi_q & -\sin\phi_{q'}\cos\phi_q \\ -\cos\phi_{q'}\sin\phi_q & \cos\phi_{q'}\cos\phi_q\end{pmatrix}. \tag{30}$$

Correspondingly, we obtain

$$\begin{aligned}\langle \boldsymbol{\sigma}', q', u'|\, c_{m,\mu}\hat{H}_{\text{vib}}\, |\boldsymbol{\sigma}, q, u\rangle - \sigma_{m,\mu}\, \langle \boldsymbol{\sigma}', q', u'|\, \hat{H}_{\text{vib}}\, |\boldsymbol{\sigma}, q, u\rangle \\ = -\, \langle \boldsymbol{\sigma}'|\boldsymbol{\sigma}\rangle\, \frac{\hbar\Omega_\mu X_\mu}{N} e^{-i(q'-q)m}[\boldsymbol{v}_{q',q}]_{u',u} + \langle \boldsymbol{\sigma}'|\boldsymbol{\sigma}\rangle\, \delta_{q',q}\delta_{u',u}\hbar\Omega_\mu\sigma_{m,\mu} + \langle \boldsymbol{\sigma}'|\boldsymbol{\sigma}\rangle\, \delta_{q',q}\delta_{u',u}\frac{\partial}{\partial {\sigma'_{m,\mu}}^{*}} H_{\text{bath}}(\boldsymbol{\sigma}'^{*}, \boldsymbol{\sigma}).\end{aligned} \tag{31}$$

Equations (18) and (19) after substitution of the results of Eqs. (20) and (21) and (29) and (31) give rise to the complete set of equations of motion for the polariton wave function. The obtained equations, however, are overcomplicated and even their numeric solution can be difficult. To proceed we appeal to the multiconfiguration Hartree framework [57]. The multiconfiguration Hartree approach is the method restructuring the set of equations of motion obtained in the time-dependent basis set. The rigorous approach to the generic solution is discussed in [55]. In our particular model [Eqs. (18) and (19)] we end up with the equations similar to the equations of the mean-field Hartree theory.

Equation (18) contains integration over $\boldsymbol{\sigma}$ inside the window cut in the narrow vicinity of $\boldsymbol{\sigma}'$. Structurally, the equation can be presented as follows:

$$\sum_{\boldsymbol{\sigma}} \langle \boldsymbol{\sigma}'|\boldsymbol{\sigma}\rangle \left[\bar{S}(\boldsymbol{\sigma}, q', u') + \sum_{m,\mu}({\sigma'_{m,\mu}}^{*} - \sigma^{*}_{m,\mu})\bar{\bar{S}}(m, \mu; \boldsymbol{\sigma}, q', u')\right] = 0. \tag{32}$$

The explicit forms of the coefficients in Eq. (32) are

$$\begin{aligned}\bar{S}(\boldsymbol{\sigma}, q', u') \equiv -\dot{\mathcal{C}}(\boldsymbol{\sigma}, q', u'|t) - i\mathcal{C}(\boldsymbol{\sigma}, q', u'|t)[(1-u')\Lambda_{-q} + u'\Lambda_{+q}] + i\sum_{q,u}\sum_{m,\mu}\frac{\Omega_\mu X_\mu}{N}(\sigma^{*}_{m,\mu} + \sigma_{m,\mu})e^{-i(q'-q)m} \\ \times [\boldsymbol{v}_{q',q}]_{u',u}\mathcal{C}(\boldsymbol{\sigma}, q, u|t) - \frac{i}{\hbar}\mathcal{C}(\boldsymbol{\sigma}, q', u'|t)H_{\text{bath}}(\boldsymbol{\sigma}^{*}, \boldsymbol{\sigma}) - i\mathcal{C}(\boldsymbol{\sigma}, q', u'|t)\sum_{m,\mu}\Omega_\mu\sigma^{*}_{m,\mu}\sigma_{m,\mu} \\ + \frac{1}{2}\mathcal{C}(\boldsymbol{\sigma}, q', u'|t)\sum_{m,\mu}[\sigma_{m,\mu}\dot{\sigma}^{*}_{m,\mu} - \sigma^{*}_{m,\mu}\dot{\sigma}_{m,\mu}],\end{aligned} \tag{33}$$

$$\bar{\bar{S}}(m,\mu;\boldsymbol{\sigma},q',u') \equiv i\sum_{q,u}\frac{\Omega_\mu X_\mu}{N}e^{-i(q'-q)m}[\boldsymbol{v}_{q',q}]_{u',u}\mathcal{C}(\boldsymbol{\sigma},q,u|t) - \mathcal{C}(\boldsymbol{\sigma},q',u'|t)\dot{\sigma}_{m,\mu}$$
$$- i\mathcal{C}(\boldsymbol{\sigma},q',u'|t)\Omega_\mu\sigma_{m,\mu} - \frac{i}{\hbar}\mathcal{C}(\boldsymbol{\sigma},q',u'|t)\frac{\partial}{\partial\sigma'^{*}_{m,\mu}}H_{\text{bath}}(\boldsymbol{\sigma}'^{*},\boldsymbol{\sigma}). \tag{34}$$

The structure of the second equation (19) is similar to that of Eq. (32) up to the integration measure. The equation in terms of the above introduced functions [Eqs. (33) and (34)] reads as

$$\sum_{\boldsymbol{\sigma}}\langle\boldsymbol{\sigma}'|\boldsymbol{\sigma}\rangle\,\mathcal{C}^*(\boldsymbol{\sigma}',q',u'|t)\left[\bar{\bar{S}}(m,\mu;\boldsymbol{\sigma},q',u') + \sigma_{m,\mu}\bar{S}(\boldsymbol{\sigma},q',u') + \sigma_{m,\mu}\sum_{n,\nu}({\sigma'_{n,\nu}}^{*} - \sigma^*_{n,\nu})\bar{\bar{S}}(n,\nu;\boldsymbol{\sigma},q',u')\right] = 0. \tag{35}$$

The integration domain in Eqs. (32) and (35) is defined by the scalar product of the coherent states $\langle\boldsymbol{\sigma}'|\boldsymbol{\sigma}\rangle = \exp(-\sum_{m,\mu}|\sigma'_{m,\mu} - \sigma_{m,\mu}|^2/2)$. Due to the large total number of the oscillators this product cuts a very narrow region in the whole configuration space. In the semiclassical approximation we set $\langle\boldsymbol{\sigma}'|\boldsymbol{\sigma}\rangle = \delta(\boldsymbol{\sigma}' - \boldsymbol{\sigma})$, so that the resulting set of equations read as $\bar{S}(\boldsymbol{\sigma},q',u') = 0$ and $\bar{\bar{S}}(m,\mu;\boldsymbol{\sigma},q',u') = 0$. The same set of equations can be obtained from the assumption that the terms $\bar{S}$ and $\bar{\bar{S}}$ nullify independently. Remarkably, this solution exhausts all possible solutions. Here is the sketch of the proof. First, we formally convert the integral equations (32) and (35) into a matrix form. For that we are indexing by integer numbers the nonintersecting domains of $\boldsymbol{\sigma}$ and replace the integration by summation. Also, we enumerate all possible couples of the vibration indices (m,μ) and of the polariton states (q',u'). The matrix of the coefficients of the obtained system of linear equations (the variables are $\bar{S}$ and $\bar{\bar{S}}$) is quadratic and, generically, its determinant is nonzero. This immediately means that only trivial solution satisfies the equations. The determinant can become zero if one or several coefficients $\mathcal{C}(\boldsymbol{\sigma},q',u'|t)$ are equal to zero. Obviously, when all coefficients $\mathcal{C}(\boldsymbol{\sigma},q',u'|t)$ are equal to zero there is no polariton excited and the vibration degrees of freedom behave independently, which problem is out of our attention. Now we show that the solution with the nonzero $\mathcal{C}(\boldsymbol{\sigma},q',u'|t)$ is self-consistent solution of the system. By equating $\bar{S}(\boldsymbol{\sigma},q',u') = 0$ we obtain the first equation of motion

$$\mathcal{C}(\boldsymbol{\sigma},q',u'|t)\left[\dot{\sigma}_{m,\mu} + i\Omega_\mu\sigma_{m,\mu} + \frac{i}{\hbar}\frac{\partial}{\partial\sigma'^{*}_{m,\mu}}H_{\text{bath}}(\boldsymbol{\sigma}'^{*},\boldsymbol{\sigma})\right] = i\frac{\Omega_\mu X_\mu}{N}\sum_{q,u}e^{-i(q'-q)m}[\boldsymbol{v}_{q',q}]_{u',u}\mathcal{C}(\boldsymbol{\sigma},q,u|t). \tag{36}$$

The other condition $\bar{\bar{S}}(m,\mu;\boldsymbol{\sigma},q',u') = 0$ yields the second equation of motion

$$\dot{\mathcal{C}}(\boldsymbol{\sigma},q',u'|t) = -i\mathcal{C}(\boldsymbol{\sigma},q',u'|t)[(1-u')\Lambda_{-q} + u'\Lambda_{+q}] + i\sum_{q,u}\sum_{m,\mu}\frac{\Omega_\mu X_\mu}{N}(\sigma^*_{m,\mu} + \sigma_{m,\mu})e^{-i(q'-q)m}[\boldsymbol{v}_{q',q}]_{u',u}\mathcal{C}(\boldsymbol{\sigma},q,u|t)$$
$$-\frac{i}{\hbar}\mathcal{C}(\boldsymbol{\sigma},q',u'|t)H_{\text{bath}}(\boldsymbol{\sigma}^*,\boldsymbol{\sigma}) - i\mathcal{C}(\boldsymbol{\sigma},q',u'|t)\sum_{m,\mu}\Omega_\mu\sigma^*_{m,\mu}\sigma_{m,\mu} + \frac{1}{2}\mathcal{C}(\boldsymbol{\sigma},q',u'|t)\sum_{m,\mu}[\sigma_{m,\mu}\dot{\sigma}^*_{m,\mu} - \sigma^*_{m,\mu}\dot{\sigma}_{m,\mu}]. \tag{37}$$

Consider the first consequence of the formulated equations [(36) and (37)]: a special combination of the equations, which generates the equation for the time evolution of the squared amplitude $|\mathcal{C}(\boldsymbol{\sigma},q',u'|t)|^2$, yields

$$\frac{\partial}{\partial t}|\mathcal{C}(\boldsymbol{\sigma},q',u'|t)|^2 = i\sum_{q,u}[\boldsymbol{v}_{q',q}]_{u',u}[\mathcal{C}(\boldsymbol{\sigma},q',u'|t)\alpha^*(q'-q)\mathcal{C}^*(\boldsymbol{\sigma},q,u|t) - \mathcal{C}^*(\boldsymbol{\sigma},q',u'|t)\alpha(q'-q)\mathcal{C}(\boldsymbol{\sigma},q,u|t)] \tag{38}$$

with the electron-vibration coupling $\alpha(q'-q)$ given by the expression

$$\alpha(q'-q) \equiv \frac{1}{N}\sum_m \alpha_m e^{-i(q'-q)m}, \tag{39}$$

$$\alpha_m \equiv \sum_\mu \Omega_\mu X_\mu(\sigma^*_{m,\mu} + \sigma_{m,\mu}). \tag{40}$$

At the derivation of Eq. (38) it has been assumed that the bath Hamiltonian is linear in $\sigma_{m,\mu}$, which is the standard form of the phonon interaction Hamiltonian. The obtained equation [Eq. (38)], in particular, shows that the amplitudes $|\mathcal{C}(\boldsymbol{\sigma},q',u'|t)|$ for all allowed values of q get nonzero values as soon as any of α_m has a nonzero value. This finishes the proof that the nonzero coefficients $\mathcal{C}(\boldsymbol{\sigma},q',u'|t)$ generate a self-consistent solution of the system (32) and (35).

One more critical condition follows from Eq. (38): it is conservation of the total probability of finding polariton in any of the allowed states. Indeed, since $\alpha^*(q'-q) = \alpha(q-q')$ and due to the symmetry of the matrix $v_{q,q'}$ ($[v_{q,q'}]_{u,u'} = [v_{q',q}]_{u',u}$) after summation over q' and u' we immediately derive

$$\dot{\mathcal{N}}(t|\boldsymbol{\sigma}) = 0, \quad \mathcal{N}(t|\boldsymbol{\sigma}) = \sum_{q,u}|\mathcal{C}(\boldsymbol{\sigma},q,u|t)|^2. \tag{41}$$

The total probability conservation allows us to sum up the equations (36) over q' and u' after multiplication of each of them by the corresponding coefficient $\mathcal{C}^*(\boldsymbol{\sigma},q',u'|t)$. In such a way we derive the equation of motion for the (m, μ) oscillator

$$\dot{\sigma}_{m,\mu} = -i\Omega_\mu \sigma_{m,\mu} + i\frac{\Omega_\mu X_\mu}{N}\chi_m(t|\boldsymbol{\sigma}) - \frac{i}{\hbar}\frac{\partial}{\partial {\sigma'}^*_{m,\mu}} H_{\text{bath}}(\boldsymbol{\sigma}'^*, \boldsymbol{\sigma}). \tag{42}$$

This equation contains the mean-field Hartree term $i\frac{\Omega_\mu X_\mu}{N}\chi_m(t|\boldsymbol{\sigma})$, which describes influence of the polariton field on the quantum oscillators. The Hartree term amplitude is

$$\chi_m(t|\boldsymbol{\sigma}) = \sum_{q',q,u',u} e^{-i(q'-q)m}[\boldsymbol{v}_{q',q}]_{u',u}\,\rho\left(t\,\middle|\,\begin{matrix} q, u \\ q', u' \end{matrix}\,\middle|\,\boldsymbol{\sigma}\right), \tag{43}$$

where ρ is the density matrix

$$\rho\left(t\,\middle|\,\begin{matrix} q, u \\ q', u' \end{matrix}\,\middle|\,\boldsymbol{\sigma}\right) = \frac{\mathcal{C}^*(\boldsymbol{\sigma}, q', u'|t)\,\mathcal{C}(\boldsymbol{\sigma}, q, u|t)}{\mathcal{N}(t|\boldsymbol{\sigma})}. \tag{44}$$

The symmetry $[v_{q,q'}]_{u,u'} = [v_{q',q}]_{u',u}$ guarantees that χ_m is a real-valued function, i.e., $\chi^*_m(t|\boldsymbol{\sigma}) = \chi_m(t|\boldsymbol{\sigma})$.

At the final step we substitute $\dot{\sigma}_{m,\mu}$ from Eq. (42) into Eq. (37) to obtain the second equation of motion

$$\begin{aligned}\dot{\mathcal{C}}(\boldsymbol{\sigma}, q', u'|t) = &-i[(1-u')\Lambda_{-q'} + u'\Lambda_{+q'})]\mathcal{C}(\boldsymbol{\sigma}, q', u'|t)\\ &- \frac{i}{2N}\mathcal{C}(\boldsymbol{\sigma}, q', u'|t)\sum_m \alpha_m \chi_m(t|\boldsymbol{\sigma})\\ &+ i\sum_{q,u}\alpha(q'-q)[\boldsymbol{v}_{q',q}]_{u',u}\mathcal{C}(\boldsymbol{\sigma}, q, u|t).\end{aligned} \tag{45}$$

Equation (45) together with Eq. (42) form a system of equations of vibration-assisted polariton motion. Deriving the equations, we did not make any approximations.

To investigate influence of the Hartree term in the next section we consider two problems: we calculate the polariton luminescence using the diagonal approximation in the equations of motion (Sec. III A); and solve the equations of motion in the vicinity of AP (Sec. III B).

III. SOLUTION OF POLARITON EQUATIONS IN VARIOUS REGIMES

It is instructive to investigate the influence of the nonlinear Hartree term in a somewhat simplified setup. To this end, we consider two types of problems, namely, we calculate the fluorescence spectra in the regime of large Rabi splitting when some sort of linearization of the equations of motion is possible (Sec. III A). Second, in Sec. III B we consider the evolution of the polariton wave function in the AP vicinity, when nonlinearity plays a crucial role.

A. Fluorescent spectrum in quasidiagonal approximation

1. Equations of motion at large Rabi splitting in the quasidiagonal approximation

In the quasidiagonal approximation one keeps only the diagonal terms $q' = q$ corresponding to the largest value of the vibational perturbation [28] in the second equation of motion [Eq. (45)]. The processes with $q \neq q'$ describe the polariton relaxation along the dispersion curve. In our consideration we neglect such processes assuming that they are much slower than any other process under consideration, so we make use the replacement $\alpha(q'-q) \to \alpha(0)$ in Eq. (45). We return back to the discussion of this issue at the end of Sec. III A 2. In addition, we consider the regime of the large Rabi splitting, i.e., when the difference $\Lambda_{-q} - \Lambda_{+q}$ is larger of all relevant characteristic frequencies of the problem. In this case, the terms describing the exchange between the polariton branches can be neglected. Using explicit form of the diagonal entries of the matrix $\boldsymbol{v}$ [Eq. (30)], which are the electronic Hopfield coefficients $\sin^2\phi_q$ and $\cos^2\phi_q$ corresponding to the upper and lower polariton branches, respectively, we obtain

$$\dot{\mathcal{C}}(\boldsymbol{\sigma}, q, 0|t) = -i\left(\Lambda_{-q} - 2\alpha(0)\left[\cos^2\phi_q - \frac{1}{2}\sum_q(\sin^2\phi_q|\mathcal{C}(\boldsymbol{\sigma}, q, 1|t)|^2 + \cos^2\phi_q|\mathcal{C}(\boldsymbol{\sigma}, q, 0|t)|^2)\right]\right)\mathcal{C}(\boldsymbol{\sigma}, q, 0|t), \tag{46}$$

$$\dot{\mathcal{C}}(\boldsymbol{\sigma}, q, 1|t) = -i\left(\Lambda_{+q} - 2\alpha(0)\left[\sin^2\phi_q - \frac{1}{2}\sum_q(\sin^2\phi_q|\mathcal{C}(\boldsymbol{\sigma}, q, 1|t)|^2 + \cos^2\phi_q|\mathcal{C}(\boldsymbol{\sigma}, q, 0|t)|^2)\right]\right)\mathcal{C}(\boldsymbol{\sigma}, q, 1|t). \tag{47}$$

The factor 2 at $\alpha(0)$ appears due to the symmetry $q \to -q$. The factors with the opposite momenta contribute identically.

To estimate the time dependence of $\alpha(0)$ we return back to Eq. (42). Instead of solving all equations for $\sigma_{m,\mu}$ independently we replace the Hartree m-dependent term χ_m [Eqs. (43) and (44)] by its average value, an m-independent approximate polariton field acting on each molecule identically. For that we use the diagonal approximation and omit the highly oscillating terms in the same way as we did in the solutions (46) and (47). These approximations are identical to the "maximal action" approximation, when one replaces χ_m by the exact upper border of its estimator (see Appendix B). Therefore, the approximate equations for the function $\sigma_{m,\mu}$ become

$$\begin{aligned}\dot{\sigma}_{m,\mu} \approx &-i\Omega_\mu\sigma_{m,\mu} - 2i\gamma\,\text{Im}\sigma_{m,\mu} - i\xi_m(t) + i\Omega_\mu X_\mu\\ &\times\sum_q(\sin^2\phi_q|\mathcal{C}(\boldsymbol{\sigma}, q, 1|t)|^2 + \cos^2\phi_q|\mathcal{C}(\boldsymbol{\sigma}, q, 0|t)|^2).\end{aligned} \tag{48}$$

Here we modeled the bath degrees of freedom by some damping with the rate γ and by a stochastic force $\xi_m(t)$. Equation (48) is the Langevin equation with an external force. Following the standard procedure we assume that the noise $\xi_m(t)$ is Gaussian with zero mean value. We imply that the noise is δ correlated in time, i.e., $\langle\xi_m(t)\xi_n(\tau)\rangle = \gamma\Omega_\mu k_B T(\delta_{m,n} + R_{m,n})\delta(t-\tau)$ ($k_B T$ is the bath temperature expressed in the energy units) and $R_{m,n}$ generates some (small) correlations between the molecules. We make the stochastic averaging in the regime when the equilibration of the vibrations happens very fast after the optical excitation. For the case of overdamped oscillator the averaged over the noise function $\sigma_{m,\mu}$ is easy to calculate, it is

$$\left\langle \sum_m (\sigma^*_{m,\mu} + \sigma_{m,\mu}) \right\rangle = 2NX_\mu \sum_q (\sin^2\phi_q |\mathcal{C}(\boldsymbol{\sigma}, q, 1|t)|^2 + \cos^2\phi_q |\mathcal{C}(\boldsymbol{\sigma}, q, 0|t)|^2), \qquad (49)$$

which means that the averaged $\langle\alpha(0)\rangle$ is proportional to the Hartree term

$$\langle\alpha(0)\rangle \equiv \left\langle \frac{1}{N}\sum_m \alpha_m \right\rangle = \omega_{\rm St} \sum_q (\sin^2\phi_q \times |\mathcal{C}(\boldsymbol{\sigma}, q, 1|t)|^2 + \cos^2\phi_q |\mathcal{C}(\boldsymbol{\sigma}, q, 0|t)|^2). \qquad (50)$$

Reformulation of the stochastic equation [Eq. (48)] in terms of the Fokker-Planck equation and consequent application of the theorem for a sums of weighted normally distributed random variables allows us to write the distribution for $\alpha(0)$ as [28]

$$P(\alpha(0)) = \sqrt{\frac{1}{2\pi k_N \omega_{\rm St} k_B T}}\, e^{-\frac{[\alpha(0) - \langle\alpha(0)\rangle]^2}{2k_N\omega_{\rm St}k_BT}}, \qquad (51)$$

where

$$k_N = \left(N + 2\sum_{i<j}^N r_{ij}\right) \Big/ N^2, \qquad (52)$$

$0 \leqslant r_{ij} \leqslant 1$ are the correlation coefficients that are different from zero when the vibrations include both the intramolecular and the intermolecular ones [see the definition of the stochastic force $\xi_m(t)$ in the paragraph between Eqs. (48) and (49)]. The assumption of the intramolecular nature of the optically active vibrations means that, in this case, they are statistically independent, so that the coefficient k_N equals $1/N$. In the other extreme case when the optically active vibrations are intermolecular ones, the correlation coefficients $r_{ij} = 1$ and $k_N = 1$.

2. *Luminescence spectrum calculation*

In an experiment, the polariton system is irradiated by the pumping light and emits light which carries information about the polariton states. The pronounced advantage of the polariton devices is the one-to-one correspondence between the polariton states and the emitted photons. Since the emitted photon is a part of the polariton particle it preserves the polariton energy and the in-plane wave vector. A fixed polariton decay rate makes it possible studying of the dynamics of these composite particles.

Formally, to relate the outer field with the intracavity one, we appeal to the quasimode approximation [58], when the in-out coupling conserves the in-plane components $q_\parallel$ of the intracavity wave vector $q = (q_\parallel, q_z)$ (see Fig. 1). The z components of the wave vector in free space are determined by the emitted photon energy. Thus, to denote the external electromagnetic field components (emitted photons) one can use solely the wave-vector component $q_\parallel$ [26,59,60]. The luminescence signal amplitude $S_{q_\parallel}(\omega)$ detected out of the sample and coming from the direction marked by the wave vector $q_\parallel$, which frequency $\omega_{\tilde{q}} = \frac{c}{n_0}|\tilde{q}|$ is generally calculated from the two-time correlation function of the quantized electric field generated by the leakage of photons (with the characteristic rate κ) through the mirrors of the microcavity [61]. The details of the calculation are given in Appendix A. The signal amplitude $S_{q_\parallel}(\omega)$ is expressed in terms of the Fourier transform of the quantum correlation functions $G_1(\omega, \omega_3)$ and $G_2(\omega, \omega_3)$ [Eqs. (A12) and (A13)]:

$$S_{q_\parallel}(\omega) \propto \hbar\omega \frac{\bar{r}_{ex}^2 \kappa^2}{\pi} {\rm Re} \int_{-\infty}^{+\infty} d\omega_3 \langle (G_1(-\omega, \omega_3) G_2(\omega, -\omega_3) + G_1^*(\omega, \omega_3) G_2^*(-\omega, -\omega_3)) \rangle, \qquad (53)$$

where the frequency ω coincides with the frequency of the wave freely propagating in the outer space. The coefficients κ and $\bar{r}_{\rm ex}$ are the effective rates of the polariton decay and creation, respectively. In addition to the quantum average of the correlation functions, we also perform the thermodynamic average, which is denoted by $\langle \ldots \rangle$. The quantum correlation function $\langle 0| P_{q_0} T e^{i\int_{t_0}^{\tau_1} \hat{\mathcal{H}}(\tau) d\tau/\hbar} A_q^\dagger |0\rangle$, entering the functions $G_1(\omega, \omega_3)$ and $G_2(\omega, \omega_3)$ [Eqs. (A12) and (A13)], describes evolution of the wave function of a polariton created with the wave vector q_0 at some instant of time t_0. The polariton evolves up to the time τ_1 when it is annihilated at the state with the wave vector q. Schematically, the process is depicted by the diagram shown in Fig. 2. The equations connecting the material and the polariton operators [Eqs. (3) and (4)] allow us to express the field operator A_q in terms of the operators P_q and Q_q. Assuming, at the moment, that only the lower branch is excited we use the replacement $A_q \to \sin\phi_q P_q$. Calculation of the spectrum essentially depends on the particularities of the polariton creation process. To specify it, we focus on the process when the polaritons are created by a short light pulse at the instant of time t_0 with the initial distribution $\mathcal{F}_u(q)$ (the subscript u stands for the lower $u = 0$ and the upper $u = 1$ branch). Therefore, after simplification the expression for the signal reduces to

$$S_{q_\parallel}(\omega) \propto \hbar\omega \bar{r}_{ex}^2 \kappa^2 \langle G(\omega) G^*(\omega) \rangle,$$
$$G(\omega) = \int_{t_0}^{+\infty} d\tau_1 e^{i\omega\tau_1} \mathcal{C}(\boldsymbol{\sigma}, q, 0|\tau_1), \qquad (54)$$

where $\mathcal{C}(\boldsymbol{\sigma}, q, 0|\tau_1)$ is the solution of the polariton equations of motion with the initial condition $\mathcal{C}(\boldsymbol{\sigma}, q, u|t_0) = \mathcal{F}_u(q)$. The factor $\sin^2\phi_q$ in Eq. (54) was included into the parameters $\bar{r}_{ex}^2\kappa^2$.

In the diagonal approximation the evolution of the polariton expansion coefficient is defined by Eqs. (46) and (47). From these equations, it follows immediately that the amplitude of the wave function is conserved, while the time dependence is contained solely in the phase factor. Thus, the

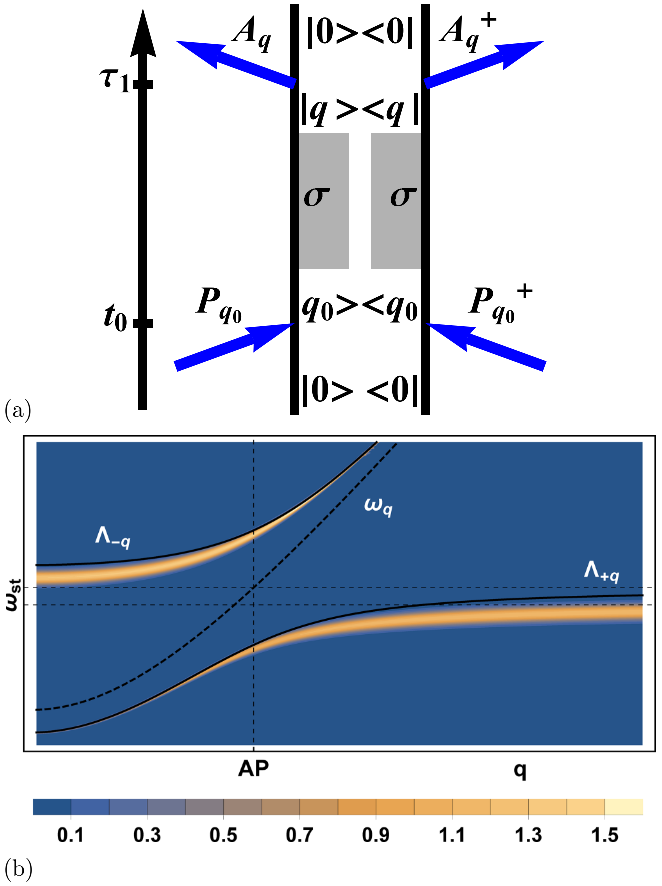

FIG. 2. (a) The ladderlike diagram depicting the contribution to the fluorescent signal [Eq. (A11)]: two polaritons (vertical lines), initially (at time t_0) created in the conjugated states with the momentum q_0 (operators P_{q_0} and $P^\dagger_{q_0}$), evolve due to interaction with the vibrational bath (the region denoted by σ) to the states with the momentum q and decay into intracavity photons (operators A_q and $A^\dagger_q$). The system's initial and final states are the vacuum states $|0\rangle$. (b) Pictorial representation of the cavity polariton fluorescence intensity (in arbitrary units) plotted vs the luminescence frequency ω and the wave vector q in the assumption that the polariton is excited at a single q, i.e., $\mathcal{F}_0(q')=\frac{1}{\sqrt{2}}(\delta_{q,q'}+\delta_{q,-q'})$ and $\mathcal{F}_1(q')=0$ in Eq. (58) for the lower polariton branch when the radiation is measured at the same q. The upper polariton branch is plotted by analogy. The dispersion curves of the cavity photons ω_q and the polariton dispersion curves $\Lambda_{\pm q}$ are shown for comparison. In the numerics we used the parameters $\omega_0=3.1\,\text{eV}$, $\omega_{\text{St}}=0.15\,\text{eV}$, $g=0.5\,\text{eV}$, $k_Nk_BT=0.03\,\text{eV}$, the dispersions $\Lambda_{\pm q}$ [Eq. (2)] are calculated with the substitution $\omega_{\text{ex}}=\omega_0+\omega_{\text{St}}/2$.

formal solution is given by

$$\mathcal{C}(\boldsymbol{\sigma},q,0|t)=\mathcal{F}_0(q)e^{-i\Lambda_{-q}(t-t_0)+i|u_q|^2\int_{t_0}^{t}\alpha(0|\tau)d\tau}, \tag{55}$$

where for convenience we introduced the notation for the effective lower branch Hopfield coefficient

$$|u_q|^2\equiv 2\left[\cos^2\phi_q-\frac{1}{2}\sum_{q'}\cos^2\phi_{q'}\mathcal{F}_0^2(q')\right]. \tag{56}$$

Therefore, in the regime of thermal equilibrium of the vibration subsystem the function $G(\omega)$ can be immediately calculated to give

$$G(\omega)=\frac{ie^{i\omega t_0}\mathcal{F}_0(q)}{\omega-\Lambda_{-q}+|u_q|^2\alpha(0)+i\bar{\gamma}}, \tag{57}$$

where the small parameter $\bar{\gamma}$ is introduced for regularization of the integrals. After averaging with the probability measure (51) we eventually derive

$$S_{q_\parallel}(\omega)\propto\sqrt{\frac{\pi}{2k_N\omega_{st}k_BT}}\frac{\hbar\omega\bar{r}_{\text{ex}}^2\kappa^2\mathcal{F}_0^2(q)}{|u_q|^2}\times\exp\left[-\frac{(\omega-\Lambda_{-q}+\langle\alpha(0)\rangle|u_q|^2)^2}{2k_N|u_q|^4\omega_{\text{St}}k_BT}\right]. \tag{58}$$

In the final expression for the fluorescent signal $S_{q_\parallel}(\omega)$ [Eq. (58)] shows that the frequency is distributed around the polariton frequency Λ_{-q}, which is shifted by the factor $-\langle\alpha(0)\rangle|u_q|^2$. In the quasistationary regime (i.e., when the polariton relaxation process is much slower than any other process, see the first paragraph of Sec. III A 1) we can approximate the polariton time-dependent wave-function coefficients in Eq. (50) by their initial values, so using the normalizing condition for $\mathcal{F}_u(q)$ we write

$$\langle\alpha(0)\rangle=\omega_{\text{St}}-\omega_{\text{St}}\sum_q(\cos^2\phi_q|\mathcal{F}_1(q)|^2+\sin^2\phi_q|\mathcal{F}_0(q)|^2). \tag{59}$$

Therefore, both the frequency shift and the distribution width depend on the initial population of the mode q, $\mathcal{F}_0(q)$. Equation (58) structurally reproduces the result (72) in [28], where the factor $\omega_{\text{St}}|\bar{u}_{s0}(\boldsymbol{q})|^2$ has to be replaced now by the product $\langle\alpha(0)\rangle|u_q|^2$. Therefore, our rigorous approach shows that the spectral shift is produced by the Hartree term. Notice also that the luminescence spectrum [Eq. (58)] is narrowing for the intramolecular nature of the low-frequency optically active vibrations ($k_N=1/N$) as the number of molecules N increases. The narrowing of the polariton luminescence spectrum by increasing the number of molecules was predicted in Ref. [28] and resembles the exchange (motional) narrowing in the absorption of molecular aggregates [62]. The difference lies in the nature of the interaction responsible for the exchange effects [28].

In Fig. 2(b) we plotted the numeric estimation of the polariton fluorescence for all values of q according to the obtained formulas [Eqs. (56), (58), and (59)]. We also extended our numerics for the upper polariton branch. It is assumed that the fluorescence is measured at the same wave vector q where the polariton was excited. The two limiting photonic and excitonic regimes are smoothly connected in the intermediate region.

For completeness, we investigate the obtained solution in two limiting cases. The simplest for the analysis case is the one which describes the polaritons created with a small momentum q and the initial amplitude $\mathcal{F}_0(q')=\frac{1}{\sqrt{2}}(\delta_{q,q'}+\delta_{q,-q'})$. In this case the Hopfield coefficient $\cos^2\phi_q$ is very small. Thus, the combination of factors generating the frequency shift, $-\langle\alpha(0)\rangle|u_q|^2\approx-\omega_{\text{St}}\cos^4\phi_q$ [Eqs. (50) and

(56)], is essentially suppressed by the fourth order of $\cos\phi_q$ and can be neglected. In the limit when $\cos^2\phi_q \to 0$ the spectrum formula can be further reduced by using the δ-function Gaussian representation $\delta(x) = \lim_{\beta\to 0}\frac{1}{\beta\sqrt{\pi}}e^{-(\frac{x}{\beta})^2}$. Since in the case under consideration $\Lambda_{-q} \sim \omega_q$ [see Fig. 1(b)], the system radiates at the photon frequency, i.e., $S_{q_\parallel}(\omega) \propto \hbar\omega\delta(\omega - \omega_q)$ [see the upper polariton branch at large q and the lower branch for small q on the fluorescence plot in Fig. 2(b)].

When the polariton is created in the state with large q, the lower polariton branch Hopfield coefficient $\cos^2\phi_q$ becomes very close to unity, so that the second term in Eq. (59) can be neglected. When the polariton field is initially fully concentrated at the wave vector q so that $|u_q|^2 \approx 1$. The expansion of Λ_{-q} over small $\omega_{\rm ex}/\omega_q$ and g/ω_q in the leading order gives $\Lambda_{-q} \approx \omega_{\rm ex}$, so that the central luminescence frequency Ω coincides with the exciton radiation frequency $\Omega \approx \omega_{\rm ex} - \omega_{\rm St} = \omega_0 + \omega_{\rm St}/2 - \omega_{\rm St} = \omega_0 - \omega_{\rm St}/2$. The linewidth reaches the value $k_N\omega_{\rm St}k_BT$ [see the lower polariton branch at large q and the upper branch for small q on the fluorescence plot in Fig. 2(b)].

The diagonal approximation, which we use to obtain the spectrum [Eq. (58)], obviously is not sufficient when the polariton characteristic decay time is large in comparison with the effective inverse rate of transitions between the states with various q. During this time the polariton wave-function amplitudes can spread over a large range of wave vectors. The time dependence of the amplitudes $|\mathcal{C}(\boldsymbol{\sigma}, q, u|t)|^2$ and the change in the momentum distribution can influence the luminescence spectrum. To go beyond the diagonal approximation, one can additionally equip the problem [Eqs. (46) and (47)] by the system of balance equations, which are formulated for the density matrix $\rho(q, u|q', u'; t) \equiv \mathcal{C}^*(\boldsymbol{\sigma}, q', u'|t)\mathcal{C}(\boldsymbol{\sigma}, q, u|t)$. Following the method proposed by Zwanzig [63], von Neumann's equation can be resolved for the diagonal entries of the density matrix $\rho(q, 0|q, 0; t) \equiv |\mathcal{C}(\boldsymbol{\sigma}, q, 0|t)|^2$ (see details of derivation in Appendix C). The obtained balance equation [Eqs. (C11) and (C12)] describes the evolution of the polariton quantum amplitudes. Note that von Neumann's equation does not contain the Hartree term in any explicit form. The estimation of the transition rate in the leading order yields $\sqrt{k_N\omega_{\rm St}k_BT/N}$ (see Appendix C). The small factor $\sqrt{k_N/N}$, suppressing the polariton relaxation along the dispersion curve, gives us the supporting argument in favor of our quasidiagonal approximation used for calculation of the fluorescent spectrum [Eq. (58)].

There are two more remarks. The obtained luminescence spectrum is defined as a thermal average of Green's function $G(\omega)$ [Eq. (57)]. The pure polariton (no vibrations) Green's function pole is located at the polariton energy. The correction to its value $[|u_q|^2\alpha(0)]$ can be interpreted as the polariton self-energy. Indeed, its structure repeats the typical structure of the self-energy term: it is a product of the Hartree forces $[\chi_m(t|\boldsymbol{\sigma})]$ exciting the vibrations and those that enter the amplitude $|u_q|^2$ with the characteristic interaction energy $\omega_{\rm St}$. Also, we note that at the construction of our theory we made a voluntary decision, when inserted the $\omega_{\rm St}/2$ directly into the definition of the polariton dispersion $\Lambda_{\pm q}$. This, however, can be done differently by inserting $\omega_{\rm St}/2$ into the definition of $\alpha(q)$. This should not bring any difference when the problem is solved nonperturbatively, while the perturbative approach can be sensitive to this choice especially close to the AP.

To conclude this section we note that the effect of molecular Stokes shift on polariton spectra at a strong light-matter coupling was seen and discussed in a number of experimental works [17,29,30]. It is worth noting that the theory developed in this paper and also in Ref. [28] can serve as a basis for the heuristic model formulated in Ref. [30]. The latter model [see Fig. 1(d) in Ref. [30]] qualitatively explains the effect of the increase of the Stokes shift in the resonant cavities compared to the one measured for the same material (dye-doped films R6G:PMMA) deposited on glass. Indeed, according to Eq. (58) with the substitution (59), the fluorescence signal maximum is found near the frequency $\Lambda_{-q} - \omega_{\rm St}|u_q|^2$, i.e., the polariton energy is corrected by the Stokes shift weighted with the excitonic contribution to the polariton. Moreover, our theory explains also the narrowing of the luminescence spectrum of R6G:PMMA film placed in the cavity with respect to the luminescence spectrum of the same film deposited on glass [see Fig. 3(c) in Ref. [30]]. The second moment of the polariton luminescence spectral line equals to the second moment of the molecular luminescence $(\omega_{\rm St}k_BT)$ multiplied by the factor $k_N|u_q|^4 < 1$ [Eq. (58)]. This means that there are at least two sources of the spectral line narrowing observed in Ref. [30]: the motional narrowing (when $k_N < 1$), and due to effective decrease of the excitonic component in the polariton accounted by the weight $|u_q|^4 < 1$.

B. Behavior of the polariton wave function in the vicinity of AP

In the previous section the solution of the equations of motion have been found in the regime where their linearization is possible. In this section we consider evolution of the polariton wave function in the AP vicinity, when the nonlinear terms are essential. As a simplifying condition, we use the assumption that the polariton wave function is initially activated at a single momentum mode $q = q_0$. To formulate our equations for this case in a convenient way we introduce the following notations: $C_u \equiv \mathcal{C}(\boldsymbol{\sigma}, q_0, u|t)$, $s \equiv \sin\phi_{q_0}$, $c \equiv \cos\phi_{q_0}$. We also redefine the time variable as $tg \to t$, and set $\Lambda_\pm \equiv \Lambda_{\pm q_0}/g$. At this choice the Rabi frequency becomes $(\Lambda_+ - \Lambda_-) = 1/cs \geqslant 2$. We also set $\mathcal{N}(t|\boldsymbol{\sigma}) = 2|C_1|^2 + 2|C_2|^2 = 1$, then the Hartree factor simplifies to the m-independent function of time $\chi_m(t|\boldsymbol{\sigma}) = 2|sC_1 - cC_0|^2$. The multiplier 2 arises from the identical contributions of the polariton modes with $+q_0$ and $-q_0$ due to the mirror symmetry of the dispersion curves. The equations for the components of $\boldsymbol{\sigma}$ no longer contain the m dependence and we define the dimensionless frequency shift amplitude

$$x(t) = -\frac{1}{Ng}\sum_m \alpha_m = -\frac{\alpha(0;t)}{g}. \tag{60}$$

In the case of m-independent vibrations the electron-vibration coupling $\alpha(q' - q)$ [Eq. (39)] is proportional to $N\delta_{q',q}$, so that there are no transitions between the states with various q, while the interbranch exchange still takes place. In the above simplified notations, the equations of motion [Eq. (45)] read as

$$\dot{C}_1 = -i\Lambda_+ C_1 + ix(t)|sC_1 - cC_0|^2 C_1 + 2ix(t)s(cC_0 - sC_1), \tag{61}$$

$$\dot{C}_0 = -i\Lambda_- C_0 + ix(t)|sC_1 - cC_0|^2 C_0 - 2ix(t)c(cC_0 - sC_1). \tag{62}$$

It is convenient to use the equations written in a trigonometric form. For the following reparametrization of the polariton coefficients

$$C_1(t) = \frac{1}{\sqrt{2}} e^{-i\Lambda_+ t + i\Theta(t) + i\eta(t) + i\Phi(t)} \sin\Psi(t), \tag{63}$$

$$C_0(t) = \frac{1}{\sqrt{2}} e^{-i\Lambda_- t + i\Theta(t) + i\eta(t) - i\Phi(t)} \cos\Psi(t), \tag{64}$$

the set of equations for the coupled angles Ψ and Φ reads as

$$\dot{\Psi}(t) = 2csx(t)\sin\left(\frac{t}{cs} + \Phi(t)\right), \tag{65}$$

$$\dot{\Phi}(t) = (c^2 - s^2)x(t) + 2csx(t)\cot 2\Psi(t)\cos\left(\frac{t}{cs} + \Phi(t)\right). \tag{66}$$

The equations for the other two dependent angles are

$$\dot{\Theta}(t) = x(t)(2|sC_1 - cC_0|^2 - 1), \tag{67}$$

$$\dot{\eta}(t) = \frac{2csx(t)}{\sin 2\Psi(t)}\cos\left(\frac{t}{cs} + \Phi(t)\right). \tag{68}$$

In the trigonometric form of the equations of motion, one can clearly see the dynamic formation of the infinite (impenetrable) potential barrier for the polariton phase $\Psi(t)$ and, consequently, for the polariton amplitude $\cos^2\Psi(t)$ due to presence of the $\cot 2\Psi(t)$ function in Eq. (66). This function forms a number of infinite barriers, which separate the phase space onto a set of permitted regions: $\frac{k\pi}{2} < \Psi(t) < \frac{(k+1)\pi}{2}$ with $k = 0, \pm 1, \ldots$. When $\Psi(t)$ comes close to the border of the permitted region, the cotangent function in Eq. (66) becomes significant. Then the rapidly growing phase $\Phi(t)$ changes the sign of the derivative $\dot{\Psi}(t)$ in Eq. (65). Therefore, presence of the nonlinear Hartree term in the equations of motions causes the splitting of the phase space.

The polariton wave-function symmetry with respect to the phase shift $\Psi(t) \to \Psi(t) \pm \frac{\pi}{2}k$ $(k = 1, 2, \ldots)$ trivially follows from the same type of symmetry of the amplitude $\cos^2\Psi(t)$. Physically, the role of the barrier can be described as follows. The repulsive nature of the barrier forbids the amplitude to become zero. In other words, the barrier separates the mixed polariton states from the pure states, i.e., the probability to find the system, when only the upper or the lower polariton is excited, equals to zero. This property disappears when the Hartree term is absent or when the vibration amplitude x_0 equals zero.

To demonstrate the repulsive properties of the barrier we solved Eqs. (65)–(68) numerically for the model function $x(t) = \Omega X x_0 \cos\Omega t$, corresponding to a coherent excitation of a single vibration mode as, for example, in the coherent Raman spectroscopy experimental method [64]. In other words, we assume that only a single vibration degree of freedom with the parameters Ω and X is excited with some amplitude x_0, and both the polariton subsystem and all other lower-frequency vibration modes (thermal bath) are neglected. The typical solutions of Eqs. (65)–(68) under the above choice of $x(t)$ are presented in Fig. 3. As expected, the phase space of Ψ is split onto permitted regions and the trajectory cannot cross the boundaries between the regions. For completeness we also calculated behavior of the phases $\Phi(t)$, $\Theta(t)$, $\eta(t)$. Since the largest increment of the phase $\Phi(t)$ is defined by the cotangent, the linear asymptotic behavior of $\Phi(t)$ is determined by these increments, which are regular in time due to quasiperiodicity of $\Psi(t)$. The solution for the small vibration frequency case [the case (1) in Fig. 3 with $\Omega = 0.1/cs$] is less typical. Here the short-scale dynamics is defined by the Rabi frequency $1/cs$ [the curves marked by (1) in Fig. 3], this dynamics is modulated by the oscillations of $x(t)$.

Let us switch to another regime when one optically active vibration is resonantly activated by polariton, i.e., when the Rabi splitting equals to the vibration frequency. In particular, we assume that the frequency Ω of some optically active vibration mode is in resonance with the Rabi splitting, i.e., $\Omega = \Lambda_+ - \Lambda_- = 1/cs$. The equations of motion for these optically active vibration modes without the bath terms read as [see Eq. (42)]

$$\dot{\sigma}_m = -i\Omega\sigma_m + 2i\frac{\Omega X}{N}|sC_1 - cC_0|^2. \tag{69}$$

At the initial time, before the formation of the dynamical barrier [$\sigma_m(0) = 0$], the polariton wave-function coefficients oscillate with the eigenpolariton frequencies $\Lambda_\pm$. From Eq. (69) we can independently calculate the linearly growing with time resonant term, it is

$$\sigma(t) \propto it\frac{\Omega X}{N} e^{-i\Omega t} sc\cos\Psi(0)\sin\Psi(0), \tag{70}$$

so that $\alpha(0;t)$ in Eq. (60), which is proportional to the real part of $\sigma(t)$, can reach significant values. This linear behavior at relatively large times is suppressed by the factors in Eqs. (63) and (64) proportional to $x(t)$, which eventually lead to increase of the detuning and thus constrain the resonant growth. Therefore, when the Rabi frequency is in resonant with the frequency of the vibration the model predicts dynamical formation of the barrier, which separates the mixed polariton state from the pure states through the resonant growth of the amplitude at the infinite barrier. Note also that influence of any decoherence, noise processes, and delocalization of the polariton packet in the regime of the vibronic level resonance pumping is inessential.

IV. DISCUSSION AND CONCLUSION

In this paper, we derive the set of equations of vibration-assisted polariton motion [Eqs. (45) and (42)]. To derive them

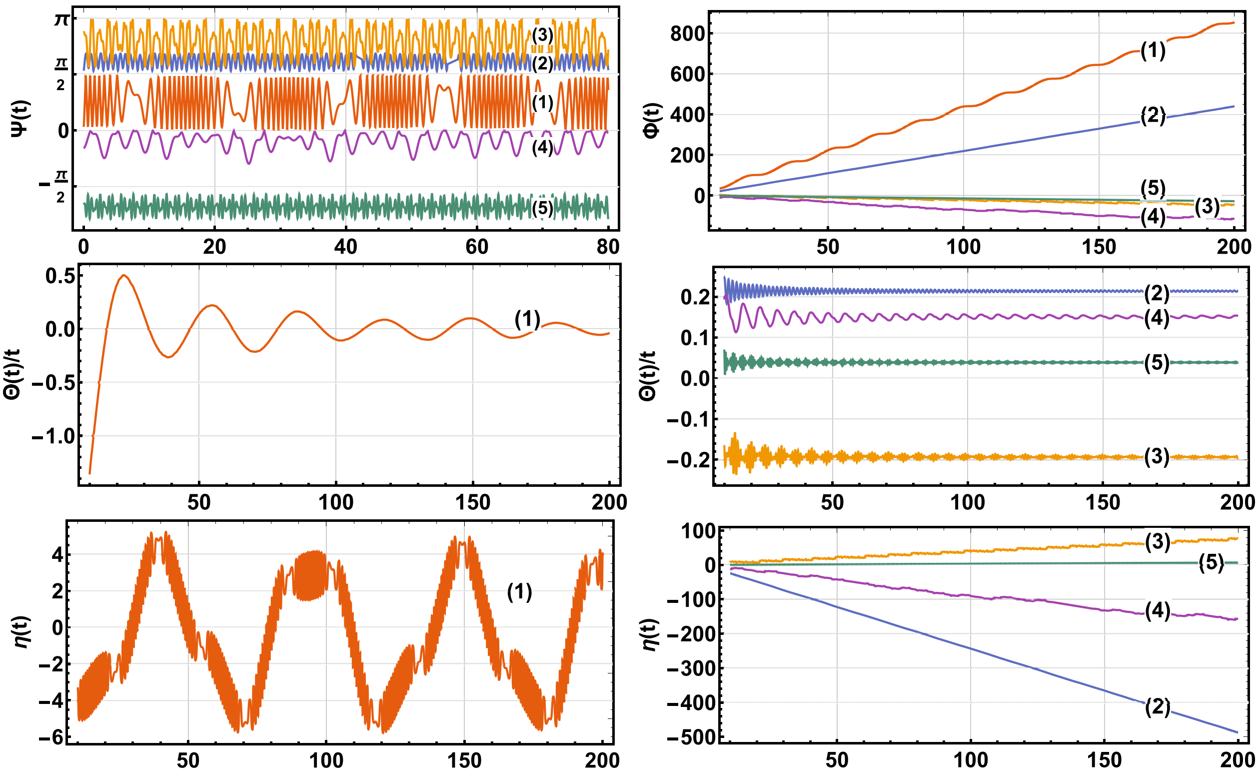

FIG. 3. The typical behavior of the phases $\Psi(t)$, $\Phi(t)$, $\Theta(t)/t$, and $\eta(t)$ in the zero-noise single-mode model. The momentum q_0 is chosen such that $\phi_{q_0} = \pi/4$, the initial phase of $\Phi(t)$ is $\tilde{\Phi}_0 = 0.1$, the other parameters are different for each case: the case (1) $\Omega = 0.1/cs$, $\Omega X x_0 = 5$, the initial phase of $\Psi(t)$ is $\tilde{\Psi}_0 = 0.1$; (2) $\Omega = 2.1/cs$, $\Omega X x_0 = 2.5$, $\tilde{\Psi}_0 = \pi/2 + 0.1$; (3) $\Omega = 3.1/cs$, $\Omega X x_0 = 5$, $\tilde{\Psi}_0 = \pi - 0.4$; (4) $\Omega = 0.5/cs$, $\Omega X x_0 = 1$, $\tilde{\Psi}_0 = -0.5$; (5) $\Omega = 5.9$, $\Omega X x_0 = 4$, $\tilde{\Psi}_0 = -\pi/2 - 0.5$.

we start from the conventional quadratic polariton Hamiltonian [Eq. (1)] and the Holstein-type vibration Hamiltonian [Eq. (8)]. The derivation method is based on the Dirac-Frenkel variation principle applied to the time-dependent basis of polariton states and on the multiconfiguration Hartree approach [55,57]. In Sec. II C we derive the set of equations of polariton motion [Eqs. (42) and (45)] and prove the correctness of the derivation procedure on the physical level of rigor. Note that the set of obtained equations for the given Hamiltonian $\hat{\mathcal{H}}$ [Eq. (7)] is in exact one-to-one correspondence with the original Schrödinger equation, no approximations were made at the derivation. Obviously, the theory becomes approximate when one goes beyond the standard harmonic oscillator approximation for the vibrations and/or includes the nonresonant light-matter interaction terms into the polariton part.

To investigate the influence of the Hartree term we considered two particular examples. In Sec. III A we estimate the polariton luminescence spectrum in the regime of large Rabi splitting and use the quasidiagonal approximation [28]. This allows us to linearize the equations of motion. Calculation of the polariton frequencies and the corresponding Hopfield coefficients is usually performed for the electronic Hamiltonian [65,66]. In this case, however, the dispersion equation for the polaritons cannot be reduced to the equation for the transverse eigenmodes of the medium [19,20,67]. To resolve this problem, the averaging of the Hopfield coefficients with respect to the low-frequency optically active vibrations has been done in Ref. [28], which made it possible to get the dispersion equation coinciding with the equation for the transverse eigenmodes. In the present approach this procedure can be performed consistently as we demonstrated in Sec. III A. The resulting spectra accurately reproduce the physical properties of the spectra [see Fig. 2(b)]. Note that the theory catches the effect of the Stokes shift in the polariton luminescence spectra. Namely, in the region of large q, where the polariton particle has a large exciton weight, the position of the luminescence maximum is redshifted by the factor ω_{St} from the position of the polariton energy Λ_{-q}. In the opposite regime, when the polariton particle is essentially a photon, the fluorescence peak coincides with the energy of the photon component of the polariton. Note also that the energy shift can be smaller than the maximal possible shift equal to ω_{St}. The shift value depends on the particular distribution of the polariton wave function in q space. The effect of molecular Stokes shift on polariton spectra for strong coupling was seen and discussed in a number of experimental works [17,29,30]. Our theory can serve as a basis for the heuristic model formulated in Ref. [30] qualitatively explaining why the Stokes shift in resonant cavities filled with R6G:PMMA is larger than that in the same dye-doped films deposited on glass. Moreover, our theory explains also the luminescence spectrum narrowing of the R6G:PMMA film in the cavity with respect to the luminescence spectrum of the same film deposited on glass [30].

Our theoretical approach originates from the theory of diabatic and adiabatic processes in quantum systems with the avoided-energy level crossing [55,57,68]. In such theories, the temporal switching between the energy branches is usually introduced through a time-dependent external parameter [68]. According to our consideration, in the polariton-vibration system, the time dependence comes from the vibrations dynamically activated by the polariton mean-field molecular. Such kind of equations are typical for the many-particle theories [55,57]. In Sec. III B we considered the polariton wave-function behavior in the vicinity of AP. In particular, we showed that when an optically active vibration is resonantly excited, the polariton particle in the AP vicinity exists only in a mixed quantum state of the upper and lower polaritons. This state is prevented from further decay into a pure upper or lower polariton state by the infinite energy barriers of a dynamical origin.

In this paper, we provide a rigorous derivation of the equations governing the vibration-assisted evolution of the polariton wave function. There are a number of special problems, which were left aside from the focus of this paper, such as revealing the vibronic progression in the polariton spectra, polariton diffusion along the dispersion curve, and the Bose-Einstein condensation description. In a more general context, our theory can be useful in the construction of rigorous approaches for the purposes of multidimensional spectroscopy [18]. Although, as noted, our theory describes the effects of molecular Stokes shift in polariton spectra at strong coupling [30], the same effects can be described within our previous approach [28]. However, the fundamental advantage of the developed here theory is in the rigorous formulation of nonlinear equations of motion. Therefore, its significance goes far beyond the explanation of the spectral Stokes shift at the strong light-matter coupling. We expect that the theory will lead us to new, associated with the nonlinearity, manifestations of the collective behavior in polaritonic and similar systems, for example, mutual synchronization of interacting oscillators, oscillation death, etc. [69]. These issues will be considered elsewhere.

ACKNOWLEDGMENTS

The work was supported by the Ministry of Science & Technology of Israel (Grant No. 79518) and by the Ariel University and the Holon Institute of Technology (Grant No. RA1900000633 for cooperative research). Authors thank H. Zoubi for useful discussions. V.O. thanks B. Gutkin for providing additional financial support. Authors thank E. Kanzieper and R. Riser for providing access to the high-performance computational resources during the initial stage of the research.

APPENDIX A: DERIVATION OF THE POLARITON FLUORESCENT SIGNAL

According to the optic version of the Wiener-Khintchine theorem, the frequency-resolved signal $S(\omega)$ is expressed in terms of the radiation field autocorrelation function

$$S(\omega) = \frac{1}{\pi}\mathrm{Re}\int_{-\infty}^{+\infty} d\tau \int_{-\infty}^{\tau} d\tau' e^{-i\omega(\tau-\tau')} \times \langle E^{(-)}(\boldsymbol{r},\tau)E^{(+)}(\boldsymbol{r},\tau')\rangle. \tag{A1}$$

The correlation function is the quantum expectation value $(\tau' < \tau)$

$$\langle E^{(-)}(\boldsymbol{r},\tau)E^{(+)}(\boldsymbol{r},\tau')\rangle = \mathrm{Tr}\,[E^{(-)}(\boldsymbol{r},\tau)E^{(+)}(\boldsymbol{r},\tau')\rho_{\mathrm{tot}}(\tau|\tau')], \tag{A2}$$

where ρ_{tot} is the density matrix of the total system, including the external field. The quantized outer electric field $E^{(\pm)}(\tilde{q},t)$, defined in the space of wave vectors $\tilde{q}$, which tangential component equals $q_{\parallel}$, is

$$E^{(-)}(\tilde{q},t) + E^{(+)}(\tilde{q},t) = -i\int d\omega \frac{\sqrt{\hbar\omega}}{c}[F_{\tilde{q}}^{\dagger}(\omega)e^{i\omega t} - F_{\tilde{q}}(\omega)e^{-i\omega t}], \tag{A3}$$

where $F_{\tilde{q}}(\omega)$ is the field operator, which also includes the dispersion relation $\delta(\omega-\omega_{\tilde{q}})$ in the outer space. The Hamiltonian term of the outer field is $H_{\mathrm{out}} = \sum_{\tilde{q}}\int d\omega\, \hbar\omega F_{\tilde{q}}^{\dagger}(\omega)F_{\tilde{q}}(\omega)$. The coupling V between the outer and the cavity light modes we describe in the minimal coupling assumption, i.e.,

$$V = i\frac{\hbar\kappa}{2\pi}\sum_{q}\int d\omega[A_q F_{\tilde{q}}^{\dagger}(\omega) - A_q^{\dagger}F_{\tilde{q}}(\omega)], \tag{A4}$$

where the photon leakage coefficient κ is assumed to be q independent. The tangential component $q_{\parallel}$ of the wave vectors $\tilde{q}$ and q coincide, while z component of q is fixed by the photon mode excited in the cavity [Fig. 1(a)] and z component of $\tilde{q}$ is determined by the emitted photon energy and by $q_{\parallel}$. Thus, the sum in Eq. (A4) effectively runs over $q_{\parallel}$.

The density matrix evolution satisfies the von Neumann's equation $\dot{\rho}_{\mathrm{tot}} = -\frac{i}{\hbar}[H_{\mathrm{out}} + V + \hat{\mathcal{H}} + H_{\mathrm{excit}}, \rho_{\mathrm{tot}}]$, which in the interaction picture transforms into the equation $\dot{\rho}_{\mathrm{tot},I} = -\frac{i}{\hbar}[V_I, \rho_{\mathrm{tot},I}]$ with

$$V_I(t|t_0) = i\frac{\hbar\kappa}{2\pi}\sum_{q}\int d\omega[A_q(t|t_0)F_{\tilde{q}}^{\dagger}(\omega)e^{-i\omega(t-t_0)} - A_q^{\dagger}(t|t_0)F_{\tilde{q}}(\omega)e^{i\omega(t-t_0)}], \tag{A5}$$

and the time-dependent photon operators

$$A_q(t|t_0) = Te^{i\int_{t_0}^{t}[\hat{\mathcal{H}}(\tau)+H_{\mathrm{excit}}(\tau)]d\tau/\hbar}A_q\; Te^{-i\int_{t_0}^{t}[\hat{\mathcal{H}}(\tau)+H_{\mathrm{excit}}(\tau)]d\tau/\hbar}. \tag{A6}$$

The H_{excit} part of the total Hamiltonian is responsible for creation of polaritons by the external classical pump field.

The density matrix expanded up to the second order over the interaction V_I is

$$\rho_{\mathrm{tot},I}(t|t_0) = \rho_{\mathrm{tot},I}^{(0)} - \frac{i}{\hbar}\int_{t_0}^{t} d\tau\big[V_I(\tau|t_0), \rho_{\mathrm{tot},I}^{(0)}\big] + \frac{1}{\hbar^2}\int_{t_0}^{t} d\tau_1\int_{t_0}^{\tau_1} d\tau_2\big[V_I(\tau_1|t_0), \big[V_I(\tau_2|t_0), \rho_{\mathrm{tot},I}^{(0)}\big]\big]. \tag{A7}$$

This expansion has to be substituted under the trace in Eq. (A2). Since the product $E^{(-)}(\boldsymbol{r},\tau)E^{(+)}(\boldsymbol{r},\tau')$ already contains the $F_q^{\dagger}F_q$ and we assume that initially the outer light modes are empty, we obtain that $\mathrm{Tr}[F_q^{\dagger}F_q\rho_{\mathrm{tot},I}^{(0)}] = 0$. The nontrivial combinations of operators has to contain the traces $\mathrm{Tr}[F_q^\dagger F_q F_q^\dagger \rho_{\mathrm{tot},I}^{(0)} F_q] = 1$. These combinations are generated by the products $F_q^\dagger F_q V_I^{(-)}(\tau_1|t_0)\rho_{\mathrm{tot},I}^{(0)} V_I^{(+)}(\tau_2|t_0)$ and $F_q^\dagger F_q V_I^{(-)}(\tau_2|t_0)\rho_{\mathrm{tot},I}^{(0)} V_I^{(+)}(\tau_1|t_0)$. The first contribution to the signal amplitude $S^1(\omega)$, measured at the position marked by the radius vector $\boldsymbol{r}$, has the form

$$S^1(\omega) = \frac{1}{2\pi\hbar}\mathrm{Re}\int_{-\infty}^{+\infty} d\tau \int_{-\infty}^{\tau} d\tau' \int d\omega_1 \sqrt{\omega_1} \int d\omega_2 e^{i\omega_1\tau} \sqrt{\omega_2} e^{-i\omega_2\tau'} e^{-i\omega(\tau-\tau')} \int_{\tau'}^{\tau} d\tau_1 \int_{\tau'}^{\tau_1} d\tau_2 \sum_{\tilde{q},\tilde{q}'} e^{i(\tilde{\boldsymbol{q}}-\tilde{\boldsymbol{q}}')\boldsymbol{r}}$$
$$\times \left[\mathrm{Tr}\ \ F_{\tilde{q}}^\dagger(\omega_1) F_{\tilde{q}'}(\omega_2) V_I^{(-)}(\tau_1|\tau')\rho_{\mathrm{tot},I}^{(0)} V_I^{(+)}(\tau_2|\tau') + \mathrm{Tr}\ \ F_{\tilde{q}}^\dagger(\omega_1) F_{\tilde{q}'}(\omega_2) V_I^{(-)}(\tau_2|\tau')\rho_{\mathrm{tot},I}^{(0)} V_I^{(+)}(\tau_1|\tau')\right]. \quad \text{(A8)}$$

Since the detector is positioned far from the sample, the major contribution to the signal comes from the terms with $\tilde{q} = \tilde{q}'$, thus the signal amplitude measured in the direction marked by a given vector $\tilde{q}$ is determined by the tangential component $q_\parallel$:

$$S_{q_\parallel}^1(\omega) = \frac{\hbar\omega_{\tilde{q}}\kappa^2}{2\pi^2}\mathrm{Re}\int_{-\infty}^{+\infty} d\tau \int_{-\infty}^{\tau} d\tau'^{-i(\omega-\omega_{\tilde{q}})(\tau-\tau')}$$
$$\times\ \mathrm{Re}\int_{\tau'}^{\tau} d\tau_1 \int_{\tau'}^{\tau_1} d\tau_2 \mathrm{Tr}\ \ F_{\tilde{q}}^\dagger(\omega_{\tilde{q}}) F_{\tilde{q}}(\omega_{\tilde{q}}) A_q^\dagger(\tau_1|\tau')$$
$$\times\ F_{\tilde{q}}^\dagger(\omega_{\tilde{q}})\rho_{\mathrm{tot},I}^{(0)} A_q(\tau_2|\tau') F_{\tilde{q}}(\omega_{\tilde{q}}) e^{-i\omega_{\tilde{q}}(\tau_1-\tau_2)}. \quad \text{(A9)}$$

After taking the trace and summing up all terms we obtain the expression

$$S_{q_\parallel}(\omega) = \frac{\hbar\omega_{\tilde{q}}\kappa^2}{\pi^2}\mathrm{Re}\int_{-\infty}^{+\infty} d\tau \int_{-\infty}^{\tau} d\tau'^{-i(\omega-\omega_{\tilde{q}})(\tau-\tau')}$$
$$\times\ \mathrm{Re}\int_{\tau'}^{\tau} d\tau_1 \int_{\tau'}^{\tau_1} d\tau_2 e^{-i\omega_{\tilde{q}}(\tau_1-\tau_2)}$$
$$\times\ \langle q,\tau'|\, A_q^\dagger(\tau_1|\tau') A_q(\tau_2|\tau')\, |q,\tau'\rangle\,. \quad \text{(A10)}$$

The quantum state $|q,\tau'\rangle$ here is a state with a previously (at instant of time τ') created polariton, which quantum amplitude has a nonzero projection onto the state with the wave vector q during the time of the polaritonic system evolution. Note that the creation of polariton is governed by the H_{excit} Hamiltonian. Its structure $H_{\mathrm{excit}} = \hbar\sum_q (r_{\mathrm{ex}}(q,t)P_q^\dagger + r_{\mathrm{ex}}^{(+)}(q,t)Q_q^\dagger) + \mathrm{c.c.}$ describes creation of the upper and the lower q polaritons with some time-dependent rates r_{ex} and $r_{\mathrm{ex}}^{(+)}$, respectively. To have a nonzero quantum average $\langle q,\tau'|\, A_q^\dagger(\tau_1|\tau') A_q(\tau_2|\tau')\, |q,\tau'\rangle$ the polariton has to be excited twice. The form of the excitation term depends on the particular realization of the excitation mechanism. Assume that the excitation happens for the lower polaritons only ($r_{\mathrm{ex}}^{(+)} \equiv 0$). Thus, explicitly, after expansion over H_{excit} we write

$$\langle q,\tau'|\, A_q^\dagger(\tau_1|\tau') A_q(\tau_2|\tau')\, |q,\tau'\rangle$$
$$= \bar{r}_{\mathrm{ex}}^2 \sum_{q'} \int_{\tau'}^{\tau_1} \frac{r_{\mathrm{ex}}(q',\tau_1')}{\bar{r}_{\mathrm{ex}}} d\tau_1' \,\langle 0|\, P_{q'} T e^{i\int_{\tau_1'}^{\tau_1} \hat{\mathcal{H}}(\tau)d\tau/\hbar} A_q^\dagger\, |0\rangle$$
$$\times \sum_{q''} \int_{\tau'}^{\tau_2} \frac{r_{\mathrm{ex}}(q'',\tau_2')}{\bar{r}_{\mathrm{ex}}} d\tau_2' \,\langle 0|\, A_q T e^{-i\int_{\tau_2'}^{\tau_2} \hat{\mathcal{H}}(\tau)d\tau/\hbar} P_{q''}^\dagger\, |0\rangle\,. \quad \text{(A11)}$$

Here we introduced a typical excitation rate constant $\bar{r}_{\mathrm{ex}}$. Such factorization [Eq. (A11)] allows us further simplification of the expression for the signal [Eq. (A10)] by taking the Fourier transform of each component,

$$G_1(\omega_2,\omega_3) = \iint_{-\infty}^{+\infty} d\tau_1 d\tau'^{i\omega_2\tau_1+i\omega_3\tau'} \sum_{q'} \int_{\tau'}^{\tau_1} d\tau_1'$$
$$\times \frac{r_{\mathrm{ex}}(q',\tau_1')}{\bar{r}_{\mathrm{ex}}} \,\langle 0|\, P_{q'} T e^{i\int_{\tau_1'}^{\tau_1} \hat{\mathcal{H}}(\tau)d\tau/\hbar} A_q^\dagger\, |0\rangle\,, \quad \text{(A12)}$$

$$G_2(\omega_4,\omega_5) = \iint_{-\infty}^{+\infty} d\tau_2 d\tau'^{i\omega_4\tau_2+i\omega_5\tau'} \sum_{q''} \int_{\tau'}^{\tau_2} d\tau_2'$$
$$\times \frac{r_{\mathrm{ex}}(q'',\tau_2')}{\bar{r}_{\mathrm{ex}}} \,\langle 0|\, A_q T e^{-i\int_{\tau_2'}^{\tau_2} \hat{\mathcal{H}}(\tau)d\tau/\hbar} P_{q''}^\dagger\, |0\rangle\,, \quad \text{(A13)}$$

such that the overall expression for the signal becomes

$$S_{q_\parallel}(\omega) = \hbar\omega\frac{\bar{r}_{\mathrm{ex}}^2\kappa^2}{\pi}\delta(\omega-\omega_{q_\parallel})\mathrm{Re}\int_{-\infty}^{+\infty} d\omega_3$$
$$\times\ (G_1(-\omega,\omega_3)G_2(\omega,-\omega_3)$$
$$+\ G_1^*(\omega,\omega_3)G_2^*(-\omega,-\omega_3)). \quad \text{(A14)}$$

At the derivation of the last expression we implied strict conservation of energy and committed the off-resonant contributions.

APPENDIX B: ESTIMATION OF THE HARTREE TERM IN EQ. (42)

The Hartree term in Eq. (42), $\frac{\Omega_\mu X_\mu}{N}\chi_m(t|\boldsymbol{\sigma})$, can be estimated from above by means of the Cauchy-Bunyakovsky-Schwarz inequality (the square of a sum is less or equal to the sum of squares). Namely,

$$\chi_m(t|\boldsymbol{\sigma}) \overset{\text{(i)}}{=} \left|\sum_q e^{iqm}(\sin\phi_q \mathcal{C}(\boldsymbol{\sigma},q,1|t) - \cos\phi_q \mathcal{C}(\boldsymbol{\sigma},q,0|t))\right|^2$$
$$\overset{\text{(ii)}}{\lesssim} \left|\sum_q e^{iqm}\sin\phi_q \mathcal{C}(\boldsymbol{\sigma},q,1|t)\right|^2$$
$$+ \left|\sum_q e^{iqm}\cos\phi_q \mathcal{C}(\boldsymbol{\sigma},q,0|t)\right|^2$$
$$\overset{\text{(iii)}}{\leqslant} N\sum_q (\sin^2\phi_q |\mathcal{C}(\boldsymbol{\sigma},q,1|t)|^2$$
$$+ \cos^2\phi_q |\mathcal{C}(\boldsymbol{\sigma},q,0|t)|^2), \quad \text{(B1)}$$

the equivalence (i) follows directly from the definitions of the Hartree force [Eqs. (43), (44), and (30)], the approximate inequality (ii) is achieved after omitting the highly oscillating terms, while the inequality (iii) represents the Cauchy-Bunyakovsky-Schwarz inequality. The latter inequality becomes close to the exact equivalence for a narrow Gaussian distribution of $\mathcal{C}(\boldsymbol{\sigma}, q, u|t)$ in the q space. The latter argument allows us to use the exact upper border as the estimator of the Hartree term χ_m (see Sec. III A 1). Note also that the diagonal approximation, i.e., when the exponential function $e^{i(q-q')m}$ is replaced by unity, ends up in the same resulting expression.

APPENDIX C: ESTIMATION OF THE TRANSITION RATE IN THE BALANCE EQUATIONS

The sum of the equation of motion [Eq. (45)] taken with the multiplier $\mathcal{C}(\boldsymbol{\sigma}, q, u|t)$ with its complex conjugation yields the equation for the density matrix $\rho(q, u|q', u'; t) = \mathcal{C}^*(\boldsymbol{\sigma}, q', u'|t)\mathcal{C}(\boldsymbol{\sigma}, q, u|t)$ of the polariton subsystem [we took into account that $\mathcal{N}(t) = 1$]. The corresponding von Neumann's equation reads as

$$\frac{\partial}{\partial t}\rho(q', u'|q, u; t) = -i\sum_{q'', u''}[h(q', u'|q'', u''; t)\rho(q'', u''|q, u; t) - \rho(q', u'|q'', u''; t)h(q'', u''|q, u; t)] \tag{C1}$$

with the Hermitian matrix $h(q', u'|q'', u''; t)$:

$$h(q', u'|q, u; t) \equiv h_0(q', u'|q, u) - h_1(q', u'|q, u; t), \tag{C2}$$

$$h_0(q', u'|q, u) \equiv [(1 - u')\Lambda_{-q'} + u'\Lambda_{+q'}]\delta_{q',q}\delta_{u',u}, \tag{C3}$$

$$h_1(q', u'|q, u; t) \equiv \alpha(q' - q)[\boldsymbol{v}_{q',q}]_{u',u}. \tag{C4}$$

The Hermiticity of $h(q', u'|q'', u''; t)$ follows from the symmetries $\alpha^*(q - q'') = \alpha(q'' - q)$ and $[\boldsymbol{v}_{q,q'}]_{u,u'} = [\boldsymbol{v}_{q',q}]_{u',u}$.

Our aim is to obtain a system of equations for the diagonal entries of the density matrix. To this end we use the method proposed by Zwanzig [63] and represent the density operator as a sum of diagonal and off-diagonal terms by means of the projection operator $\hat{D}$ [a three-dimensional tensor with the entries $\hat{D}_{m,n,k} = \delta_{m,n}\delta_{n,k}$ and satisfying the properties $\hat{D}^2 = \hat{D}$, $(\mathbb{1} - \hat{D})^2 = (\mathbb{1} - \hat{D})$], such that $\rho = \hat{D}\rho + (\mathbb{1} - \hat{D})\rho$. Using the obvious properties $\hat{D}[h, \hat{D}\rho] = [\hat{D}h, \hat{D}\rho] = 0$, which hold for any h and ρ, we obtain

$$\hat{D}\dot{\rho} = -i\hat{D}[h, (\mathbb{1} - \hat{D})\rho], \tag{C5}$$

$$(\mathbb{1} - \hat{D})\dot{\rho} = -i(\mathbb{1} - \hat{D})[h, \hat{D}\rho] -i(\mathbb{1} - \hat{D})[h, (\mathbb{1} - \hat{D})\rho]. \tag{C6}$$

It is natural to assume that the initial density matrix has the diagonal entries only, so that $(\mathbb{1} - \hat{D})\rho(0) = 0$. Therefore, the solution for $(\mathbb{1} - \hat{D})\rho(t)$ is given by the integral

$$(\mathbb{1} - \hat{D})\rho(t) = -i(\mathbb{1} - \hat{D})\int_0^t u^\dagger(\tau, t)[h(\tau), \hat{D}\rho(\tau)]u(\tau, t)d\tau, \tag{C7}$$

with the unitary matrix

$$u(\tau, t) = T\ \exp\left[-i\int_t^\tau h(\tau_1)d\tau_1\right]. \tag{C8}$$

Substitution of the expression (C7) into (C5) gives rise to the balance equations for the diagonal entries of the density matrix in the form

$$\hat{D}\dot{\rho} = -\hat{D}\int_0^t d\tau[(\mathbb{1} - \hat{D})h(t), \times u^\dagger(\tau, t)[(\mathbb{1} - \hat{D})h(\tau), \hat{D}\rho(\tau)]u(\tau, t)]. \tag{C9}$$

Having formulated the equation for the diagonal entries of the density matrix [Eq. (C9)] we have to make the thermodynamic averaging. To perform the averaging, we can assume that the vibration degrees of freedom equilibrate very fast between the optical transitions. This allows us, first, to make the factorization of the expectation value $\langle h(q', u'|q'', u''; t)\rho(q'', u''|q, u; t)\rangle = \langle h(q', u'|q'', u''; t)\rangle\langle\rho(q'', u''|q, u; t)\rangle$; second, to draw the density matrix out the time integration; and to use the limiting distribution for α_m, as in Sec. III A [Eq. (51)], which is the Gaussian distribution with some mean value $\bar{\alpha}_m$:

$$P(\alpha_m) = \frac{1}{\sqrt{2\pi N k_N \omega_{\mathrm{St}} k_B T}}\exp\left[-\frac{(\alpha_m - \bar{\alpha}_m)^2}{2N k_N \omega_{\mathrm{St}} k_B T}\right]. \tag{C10}$$

From the definition of $\langle\alpha(0)\rangle$, which is $\langle\alpha(0)\rangle = N^{-1}\sum_m \bar{\alpha}_m$, we can also approximately replace each $\bar{\alpha}_m$ by $\langle\alpha(0)\rangle$. One can show that under the above assumption the balance equation (C9) for the lower polariton branch, eventually, reduces to the form

$$\frac{d}{dt}\langle\rho(q, 0|q, 0; t)\rangle = \sum_{q'}\mathcal{K}(q, q')(\langle\rho(q, 0|q, 0; t)\rangle - \langle\rho(q', 0|q', 0; t)\rangle), \tag{C11}$$

with the time-independent kernel $\mathcal{K}(q, q')$, which is approximately calculated as

$$\mathcal{K}(q, q') \approx \left\langle\int_0^t d\tau[(\mathbb{1} - \hat{D})h(t)]_{q,q'}[(\mathbb{1} - \hat{D})h(\tau)]_{q',q} \times (u^\dagger_{q',q'}(\tau, t)u_{q,q}(\tau, t) + u_{q',q'}(\tau, t)u^\dagger_{q,q}(\tau, t))\right\rangle. \tag{C12}$$

The rough estimation of the transition rate can be done by averaging of the leading term $\frac{1}{N^2}\sum_m \alpha_m^2$ in the kernel (C12) with respect to the probability measure (C10). It gives the estimation $|\mathcal{K}(q, q')| \propto \sqrt{k_N \omega_{\mathrm{St}} k_B T/N}$.

[1] K. Takazawa, J. Inoue, K. Mitsuishi, and T. Takamasu, Fraction of a Millimeter Propagation of Exciton Polaritons in Photoexcited Nanofibers of Organic Dye, Phys. Rev. Lett. **105**, 067401 (2010).

[2] T. W. Ebbesen, Hybrid light–matter states in a molecular and material science perspective, Acc. Chem. Res. **49**, 2403 (2016).

[3] A. V. Kavokin, J. J. Baumberg, G. Malpuech, and F. P. Laussy, *Microcavities*, 2nd ed. (Oxford University Press, Oxford, 2017).

[4] M. Hertzog, M. Wang, J. Mony, and K. Börjesson, Strong light–matter interactions: a new direction within chemistry, Chem. Soc. Rev. **48**, 937 (2019).

[5] T. E. Li, J. E. Subotnik, and A. Nitzan, Cavity molecular dynamics simulations of liquid water under vibrational ultrastrong coupling, Proc. Natl. Acad. Sci. USA **117**, 18324 (2020).

[6] J. A. Hutchison, T. Schwartz, C. Genet, E. Devaux, and T. W. Ebbesen, Modifying chemical landscapes by coupling to vacuum fields, Angew. Chem. Int. Ed. **51**, 1592 (2012).

[7] M. S. Skolnick, T. A. Fisher, and D. M. Whittaker, Strong coupling phenomena in quantum microcavity structures, Semicond. Sci. Technol. **13**, 645 (1998).

[8] J. Kasprzak, M. Richard, S. Kundermann, A. Baas, P. Jeambrun, J. M. J. Keeling, F. M. Marchetti, M. H. Szymańska, R. André, J. L. Staehli, V. Savona, P. B. Littlewood, B. Deveaud, and L. S. Dang, Bose–Einstein condensation of exciton polaritons, Nature (London) **443**, 409 (2006).

[9] T. D. Doan, H. Th. Cao, D. B. T. Thoai, and H. Haug, Microcavity polariton kinetics for bosonic condensation and lasing in II-VI compound materials, Phys. Rev. B **74**, 115316 (2006).

[10] G. G. Rozenman, K. Akulov, A. Golombek, and T. Schwartz, Long-range transport of organic exciton-polaritons revealed by ultrafast microscopy, ACS Photonics **5**, 105 (2018).

[11] S. Hou, M. Khatoniar, K. Ding, Y. Qu, A. Napolov, V. M. Menon, and S. R. Forrest, Ultralong-range energy transport in a disordered organic semiconductor at room temperature via coherent exciton-polariton propagation, Adv. Mater. **32**, 2002127 (2020).

[12] V. M. Agranovich, *Excitations in Organic Solids* (Oxford University Press, New York, 2009).

[13] B. D. Fainberg, N. N. Rosanov, and N. A. Veretenov, Light-induced “plasmonic” properties of organic materials: Surface polaritons and switching waves in bistable organic thin films, Appl. Phys. Lett. **110**, 203301 (2017).

[14] M. Litinskaya, P. Reineker, and V. M. Agranovich, Fast polariton relaxation in strongly coupled organic microcavities, J. Lumin. **110**, 364 (2004).

[15] D. M. Coles, P. Michetti, C. Clark, W. Ch. Tsoi, A. M. Adawi, J.-S. Kim, and D. G. Lidzey, Vibrationally assisted polariton-relaxation processes in strongly coupled organic-semiconductor microcavities, Adv. Funct. Mater. **21**, 3691 (2011).

[16] S. Baieva, O. Hakamaa, G. Groenhof, T. T. Heikkil, and J. J. Toppari, Dynamics of strongly coupled modes between surface plasmon polaritons and photoactive molecules: The effect of the stokes shift, ACS Photonics **4**, 28 (2017).

[17] E. Hulkko, S. Pikker, V. Tiainen, R. H. Tichauer, G. Groenhof, and J. J. Toppari, Effect of molecular Stokes shift on polariton dynamics, J. Chem. Phys. **154**, 154303 (2021).

[18] D. Finkelstein-Shapiro, P.-A. Mante, S. Sarisozen, L. Wittenbecher, I. Minda, S. Balci, T. Pullerits, and D. Zigmantas, Understanding radiative transitions and relaxation pathways in plexcitons, Chem **7**, 1092 (2021).

[19] B. D. Fainberg, Mean-field electron-vibrational theory of collective effects in photonic organic materials. Long-range Frenkel exciton polaritons in nanofibers of organic dye, AIP Adv. **8**, 075314 (2018).

[20] B. D. Fainberg, Study of electron-vibrational interaction in molecular aggregates using mean-field theory: From exciton absorption and luminescence to exciton-polariton dispersion in nanofibers, J. Phys. Chem. C **123**, 7366 (2019).

[21] Y. Toyozawa, On the dynamical behavior of an exciton, Prog. Theor. Phys. Suppl. **12**, 111 (1959).

[22] M. Reitz, C. Sommer, and C. Genes, Langevin Approach to Quantum Optics with Molecules, Phys. Rev. Lett. **122**, 203602 (2019).

[23] A. Semenov and A. Nitzan, Electron transfer in confined electromagnetic fields, J. Chem. Phys. **150**, 174122 (2019).

[24] N. Wu, J. Feist, and F. J. Garcia-Vidal, When polarons meet polaritons: Exciton-vibration interactions in organic molecules strongly coupled to confined light fields, Phys. Rev. B **94**, 195409 (2016).

[25] R. J. Holmes and S. R. Forrest, Strong Exciton-Photon Coupling and Exciton Hybridization in a Thermally Evaporated Polycrystalline Film of an Organic Small Molecule, Phys. Rev. Lett. **93**, 186404 (2004).

[26] L. Mazza, L. Fontanesi, and G. C. La Rocca, Organic-based microcavities with vibronic progressions: Photoluminescence, Phys. Rev. B **80**, 235314 (2009).

[27] F. Herrera and F. C. Spano, Dark Vibronic Polaritons and the Spectroscopy of Organic Microcavities, Phys. Rev. Lett. **118**, 223601 (2017).

[28] B. D. Fainberg and V. Al. Osipov, Effects of electron–vibration interaction in polariton luminescence: Non-Markovian Fano resonances and hot luminescence, J. Phys. Chem. A **126**, 2761 (2022).

[29] D. G. Lidzey, D. D. C. Bradley, T. Virgili, A. Armitage, M. S. Skolnick, and S. Walker, Room Temperature Polariton Emission from Strongly Coupled Organic Semiconductor Microcavities, Phys. Rev. Lett. **82**, 3316 (1999).

[30] E. K. Tanyi, H. Thuman, N. Brown, S. Koutsares, V. A. Podolskiy, and M. A. Noginov, Control of the Stokes shift with strong coupling, Adv. Opt. Mater. **5**, 1600941 (2017).

[31] M. M. Glazov, H. Ouerdane, L. Pilozzi, G. Malpuech, A. V. Kavokin, and A. D’Andrea, Polariton-polariton scattering in microcavities: A microscopic theory, Phys. Rev. B **80**, 155306 (2009).

[32] B. Xiang, R. F. Ribeiro, A. D. Dunkelberger, J. Wang, Y. Li, B. S. Simpkins, J. C. Owrutsky, J. Yuen-Zhou, and W. Xiong, Two-dimensional infrared spectroscopy of vibrational polaritons, Proc. Natl. Acad. Sci. USA **115**, 4845 (2018).

[33] T. Skettrup, Microscopic approach to polaritons, Phys. Rev. B **24**, 884 (1981).

[34] A. Quattropani, L. C. Andreani, and F. Bassani, Quantum theory of polaritons with spatial dispersion: Exact solutions, Il Nuovo Cimento D **7**, 55 (1986).

[35] J. A. Cwik, S. Reja, P. B. Littlewood, and J. Keeling, Polariton condensation with saturable molecules dressed by vibrational modes, Europhys. Lett. **105**, 47009 (2014).

[36] H. C. Longuet-Higgins, U. Öpik, M. H. L. Pryce, and R. A. Sack, Studies of the Jahn-Teller effect. II. The dynamical problem, Proc. R. Soc. London A **244**, 1 (1958).

[37] B. Gu and S. Mukamel, Cooperative conical intersection dynamics of two pyrazine molecules in an optical cavity, J. Phys. Chem. Lett. **11**, 5555 (2020).

[38] M. Toutounji, G. J. Small, and S. Mukamel, Optical response functions for condensed systems with linear and quadratic electron–vibration coupling, J. Chem. Phys. **109**, 7949 (1998).

[39] J.-M. Sixdeniers and K. A. Penson, On the completeness of coherent states generated by binomial distribution, J. Phys. A: Math. Gen. **33**, 2907 (2000).

[40] D. V. Shalashilin and M. S. Child, The phase space CCS approach to quantum and semiclassical molecular dynamics for high-dimensional systems, Chem. Phys. **304**, 103 (2004).

[41] A. Szabo and N. S. Ostlund, *Modern Quantum Chemistry: Introduction to Advanced Electronic Structure Theory* (Dover, New York, 1996).

[42] T. Holstein, Studies of polaron motion: Part I. The molecular-crystal model, Ann. Phys. **8**, 325 (1959).

[43] M. C. Gather and S. H. Yun, Bio-optimized energy transfer in densely packed fluorescent protein enables near-maximal luminescence and solid-state lasers, Nat. Commun. **5**, 5722 (2014).

[44] C. P. Dietrich, A. Steude, L. Tropf, M. Schubert, N. M. Kronenberg, K. Ostermann, S. Hofling, and M. C. Gather, An exciton-polariton laser based on biologically produced fluorescent protein, Sci. Adv. **2**, e1600666 (2016).

[45] N. J. Hestand and F. C. Spano, Expanded theory of H- and J-molecular aggregates: The effects of vibronic coupling and intermolecular charge transfer, Chem. Rev. **118**, 7069 (2018).

[46] M. K. Grover and R. Silbey, Exciton-phonon interactions in molecular crystals, J. Chem. Phys. **52**, 2099 (1970).

[47] M. Ormö, A. B. Cubitt, K. Kallio, L. A. Gross, R. Y. Tsien, and S. J. Remington, Crystal structure of the "aequorea victoria" green fluorescent protein, Science **273**, 1392 (1996).

[48] M. Combescot and W. Pogosov, Microscopic derivation of Frenkel excitons in second quantization, Phys. Rev. B **77**, 085206 (2008).

[49] M. Combescot and W. Pogosov, Composite boson many-body theory for Frenkel excitons, Eur. Phys. J. B **68**, 161 (2009).

[50] V. M. Agranovich, M. Litinskaya, and D. G. Lidzey, Cavity polaritons in microcavities containing disordered organic semiconductors, Phys. Rev. B **67**, 085311 (2003).

[51] S. V. Tyablikov, *Methods in the Quantum Theory of Magnetism* (Plenum, New York, 1967).

[52] M. Litinskaya, Exciton polariton kinematic interaction in crystalline organic microcavities, Phys. Rev. B **77**, 155325 (2008).

[53] H. Zoubi, Collective interactions in an array of atoms coupled to a nanophotonic waveguide, Phys. Rev. A **89**, 043831 (2014).

[54] W. H. Miller, On the relation between the semiclassical initial value representation and an exact quantum expansion in time-dependent coherent states, J. Phys. Chem. B **106**, 8132 (2002).

[55] M. Werther and F. Großmann, Apoptosis of moving nonorthogonal basis functions in many-particle quantum dynamics, Phys. Rev. B **101**, 174315 (2020).

[56] E. Artacho and D. D. O'Regan, Quantum mechanics in an evolving Hilbert space, Phys. Rev. B **95**, 115155 (2017).

[57] U. Manthe, H. D. Meyer, and L. S. Cederbaum, Wavepacket dynamics within the multiconfiguration Hartree framework: General aspects and application to NOCI, J. Chem. Phys. **97**, 3199 (1992).

[58] V. Savona, C. Piermarocchi, A. Quattropani, P. Schwendimann, and F. Tassone, Optical properties of microcavity polaritons, Phase Transitions **68**, 169 (1999).

[59] H. Zoubi and G. C. La Rocca, Microscopic theory of anisotropic organic cavity exciton polaritons, Phys. Rev. B **71**, 235316 (2005).

[60] J. Chovan, I. E. Perakis, S. Ceccarelli, and D. G. Lidzey, Controlling the interactions between polaritons and molecular vibrations in strongly coupled organic semiconductor microcavities, Phys. Rev. B **78**, 045320 (2008).

[61] J. H. Eberly and K. Wodkiewicz, The time-dependent physical spectrum of light, J. Opt. Soc. Am. **67**, 1252 (1977).

[62] E. W. Knapp, Lineshapes of molecular aggregates, exchange narrowing and intersite correlation, Chem. Phys. **85**, 73 (1984).

[63] R. Zwanzig, On the identity of three generalized master equations, Physica (Amsterdam) **30**, 1109 (1964).

[64] G. Marowsky and V. V. Smirnov, *Coherent Raman Spectroscopy: Recent Advances* (Springer, Berlin, 1992).

[65] J. J. Hopfield, Theory of the contribution of excitons to the complex dielectric constant of crystals, Phys. Rev. **112**, 1555 (1958).

[66] J. Knoester and S. Mukamel, Polaritons and retarded interactions in nonlinear optical susceptibilities, J. Chem. Phys. **91**, 989 (1989).

[67] H. Haug and S. W. Koch, *Quantum Theory of the Optical and Electronic Properties of Semiconductors* (World Scientific, Singapore, 2001).

[68] Y. Kayanuma, Phase coherence and nonadiabatic transition at a level crossing in a periodically driven two-level system, Phys. Rev. B **47**, 9940 (1993).

[69] A. Pikovsky, M. Rosenblum, and J. Kurths, *Synchronization. A Universal Concept in Nonlinear Sciences* (Cambridge University Press, New York, 2003).